Atmos. Chem. Phys. Discuss., https://doi.org/10.5194/acp-2018-506
Manuscript under review for journal Atmos. Chem. Phys.
Discussion started: 22 June 2018

Atmospheric Chemistry and Physics Discussions

Title:

Stable isotope measurements confirm volatile organic compound oxidation as a major urban summertime source of carbon monoxide in Indianapolis, USA

Authors:

*Isaac J Vimont[1,2], Jocelyn C. Turnbull[3], Vasilii V. Petrenko[4], Philip F. Place[4], Colm Sweeney[2], Natasha Miles[5], Scott Richardson[5], Bruce H. Vaughn[1], James W.C. White[1]

1. Institute of Arctic and Alpine Research, Boulder, CO USA
2. National Oceanic and Atmospheric Administration, Global Monitoring Division, Boulder, CO USA
3. GNS Science, Lower Hutt, New Zealand
4. University of Rochester Earth and Environmental Science Department, Rochester, NY, USA
5. Pennsylvania State University, College Station, PA USA

* Corresponding Author: Isaac.vimont@colorado.edu

Abstract:

Atmospheric carbon monoxide (CO) is a regulated pollutant in urban centers. Oxidation of volatile organic compounds (VOCs) has been hypothesized to contribute substantially to the summertime urban CO budget. We performed measurements of CO stable isotopes on air samples from three sites in and around Indianapolis, USA over three summers to investigate the VOC contribution to urban CO. One of the sites is located upwind of the city, allowing us to quantitatively remove the background air signal and isolate the urban CO enhancements. The distinct isotopic signatures of CO produced from fossil fuel combustion and VOC oxidation allow us to separate contributions from these two sources. Our results provide the strongest empirical evidence to date of large contributions from VOC oxidation to the urban summertime CO source and show that this contribution varies in time and location between 0 and 58%. We attribute the remainder of the Indianapolis summertime CO budget to fossil fuel combustion. We assess the reactivities of different VOCs and determine that biogenic sources are likely

Atmos. Chem. Phys. Discuss., https://doi.org/10.5194/acp-2018-506
Manuscript under review for journal Atmos. Chem. Phys.
Discussion started: 22 June 2018

responsible for the majority of CO produced by VOC oxidation reactions within Indianapolis.

1. Introduction

On the global scale, mole fraction of carbon monoxide (CO) has four major sources which include biomass burning, oxidation of methane (CH_4), the incomplete combustion of fossil fuels and the oxidation of biogenic volatile organic compounds (BVOC's, Logan et al., 1981; Duncan et al., 2007, Table 1). These sources are countered by the oxidation of CO by hydroxyl radicals (OH) resulting in a mean residence time of CO in the atmosphere of roughly 2 months (Logan et al., 1981; Duncan et al., 2007). On a regional scale in urban areas, CO mole fractions are often significantly enhanced due to the incomplete combustion of fossil fuels (https://www.epa.gov/air-emissions-inventories/air-emissions-sources, Mak and Kra, 1999; Popa et al., 2014; Turnbull et al., 2015; Vimont et al., 2017). Additionally, during the summer months, previous literature suggests that there may be large urban source of CO from the oxidation of biogenic volatile organic compounds (BVOC's) (Guenther et al., 1993, 1995; Carter and Atkinson, 1996; Kanakidou and Crutzen, 1999).

Tangential evidence of a significant urban CO source in addition to fossil fuel combustion is provided by Turnbull et al. (2006) and Miller et al. (2012). These studies aimed to predict fossil fuel CO_2 ($CO_{2,ff}$) by using CO as a proxy gas, but noted that the ratio of $CO:CO_{2,ff}$ was higher in the summer than the winter (Turnbull et al., 2006; Miller et al., 2012). A higher $CO:CO_{2,ff}$ ratio is not consistent with a sink process, such as an increase in OH during the summer months. Instead, an increase in a non-fossil fuel source provides the most likely explanation for the increase in the $CO:CO_{2,ff}$ ratio. These studies hypothesized, but could not confirm, that oxidation of VOC's may be the source of this summertime increase in CO.

Studies that model the effect of CO sources on the measured CO mole fraction have also suggested oxidation of VOC's contribute significantly to the CO budget, in particular BVOC emissions (e.g. Kanakidou and Crutzen, 1999). Griffin et al. (2007) used an atmospheric chemistry model to investigate CO production by VOC oxidation at a regional scale in the United States. Their model determined that 20-40 nmol mol^{-1} out of an approximate enhancement of 100- 200 nmol mol^{-1} of CO in air was derived from VOC oxidation, and attributed the majority of this to isoprene. Cheng et al. (2017) measured O_3 and CO mole fractions and then modeled CO production from the various sources using O_3-to-CO ratios. Their model suggested the oxidation of isoprene might account for the total anthropogenic production of CO within the urban region of Baltimore, USA.

No matter the scale, the attribution and quantification of CO sources and sinks is difficult. Forward and inverse modeling estimates that simply use CO mole fraction measurements to apportion the relative impact of sinks and sources have high uncertainty due to additional uncertainties in transport and chemistry (e.g. Kanakidou and Crutzen, 1999; Duncan et al., 2007). Measuring stable isotopes of CO (^{13}CO and $C^{18}O$) can provide a robust method to directly quantify the relative strengths of the different sources of CO and avoid some of the complications encountered with simply modeling the CO mole fraction (Brenninkmeijer, 1993; Röckmann and Brenninkmeijer, 1997; Brenninkmeijer et al., 1999). However, accurately apportioning the various sources of CO from atmospheric observations of the isotopic content can only be done if the isotopic signatures of the sources are well known (Brenninkmeijer et al., 1999). The large differences between the signatures of different sources in both ^{13}CO and $C^{18}O$ make source attribution possible despite the substantial uncertainties associated with the isotopic signatures of the sources and the OH sink (Brenninkmeijer et al., 1999; Gros et al., 2001, 2002) (Table 1). For example, the $C^{18}O$ signature of oxidation sources (~0‰) is significantly lighter than combustion sources (16-24‰) (Brenninkmeijer et al., 1999; Gros et al., 2001; Table 1).

Only a few prior studies of CO isotopes in urban regions exist (Stevens et al., 1972; Sakagawa and Kaplan, 1997; Mak and Kra, 1999; Kato et al., 1999; Tsunogai et al., 2003; Saurer et al., 2009; Popa et al., 2014; Vimont et al., 2017). These studies generally attribute much of the urban pollution to combustion of fossil fuels via automobiles and biomass burning (Saurer et al., 2009; Kato et al., 1999). This, along with variations in fuel sources, can cause CO source isotopic signatures to change through time and differ regionally, particularly in urban areas (Popa et al., 2014).

Although none of the previous urban CO isotopic studies have identified VOC oxidation as a significant urban source of CO, Sakugawa and Kaplan (1997) noted an "unknown", non-fossil source of CO within Los Angeles, CA, USA. Stevens et al. (1972) suggest oxidized BVOC's as a source of rural CO during the spring and summer months, but attribute urban CO to engine emissions alone.

Mak and Kra (1999) found a "burst" of CO in the spring during their measurement campaign at Long Island, NY, USA, and attribute this to a rapid increase in fossil fuel combustion from tourist activity in the region and peak energy consumption during the summer months. This conclusion was based on known energy data and tourist information (Mak and Kra, 1999). However, the isotopic data presented by Mak and Kra (1999) do not preclude increased oxidation of VOC's, though the signal is complicated by the increase of OH oxidation of CO and CH_4. Vimont et al. (2017) examined the wintertime urban CO budget of Indianapolis and characterized the overall isotopic signature of CO emissions from fossil fuel combustion.

In this study, we use stable isotopes of carbon monoxide measured over two summers to assess the contribution from oxidized VOCs to the CO budget at Indianapolis. We then identify the likely CO precursors by assessing expected mixing ratios and atmospheric oxidation rates.

2. Methods

2.1 Tower Sampling at Indianapolis

Atmos. Chem. Phys. Discuss., https://doi.org/10.5194/acp-2018-506
Manuscript under review for journal Atmos. Chem. Phys.
Discussion started: 22 June 2018

Atmospheric Chemistry and Physics Discussions

Indianapolis, Indiana is a metropolitan area of over one million people in the Mid-West region of the United States. It is surrounded by mostly agriculture interspersed with trees and foliage both inside and outside of its borders (Figure 1). It has distinct seasons, with hot summers (25 to 30° C) and cold winters (-8 to 1° C), which result in a distinct growing season, with the winter being relatively devoid of biogenic fluxes of CO and CO_2 (Turnbull et al., 2015). The Indianapolis FLUX project (INFLUX) aims to develop and assess methods for determining urban greenhouse gas emissions. CO, though not a primary greenhouse gas, is measured and used as a tracer for fossil fuel CO_2 emissions, and to provide information for source attribution. This study uses CO isotope measurements on samples from the existing INFLUX network and attempts to better quantify the urban CO source budget.

INFLUX has twelve instrumented towers within and around the urban boundary (Figure 2) (Miles et al., 2017). The flask-sampling regime was described in detail by Vimont et al. (2017) and Turnbull et al. (2015). In brief, discrete air samples are collected at six of the towers, three of which are sampled for CO isotopes (towers 1 - 3 on Figure 2) approximately six days per month, during the early afternoon when the strongest boundary layer mixing occurs (19:00 UTC, 14:00 local). Stable isotope measurements of CO were made on samples collected from July 2013 to July 2015. However, this study only considers the summer samples that were collected in July and August 2013, May-August 2014, and May – July 2015 (inclusive) from tower 1 (121 m above ground level (AGL), 39.5805° N, 86.4207° W), tower 2 (136 m AGL, 39.7978° N, 86.0183° W), and tower 3 (54 m AGL, 39.7833° N, 86.1652° W) (Figure 2). NOAA's Earth System Research Laboratory (ESRL) provided the CO mole fraction measurements used in this study (Novelli et al., 2003).

For the samples in this study, collection was done when the wind was approximately from the west, so that Tower 1 provides a clean-air background for the towers further to the east (Turnbull et al., 2012). Tower 2 is east of the city,

with only a small residential influence and one major highway nearby, with significant foliage within its influence footprint (Turnbull et al., 2015; Figure 2). Tower 3 is in the downtown, urban center, and is strongly influenced by anthropogenic fossil fuel emissions, with relatively fewer biogenic sources (Turnbull et al., 2015; Figure 2). The distance between towers 1 and 2 is larger (51 km) than the distance between towers 1 and 3 (36 km). Therefore, there is more time for reactions to occur between tower 2 and tower 1, and any atmospheric reaction source of CO will have greater influence at tower 2 relative to tower 3. Figure 3 shows the tower "footprints" for several of the towers at Indianapolis, which indicate the regions of greatest influence for each tower.

The air samples are collected in Portable Flask Packages (PFP's) provided by the National Oceanic and Atmospheric Administration Global Reference Network (NOAA GRN)(https://www.esrl.noaa.gov/gmd/ccgg/aircraft/sampling.html). The samples were taken using a 15 L integrating volume with 2 compressors, a water trap to dry the sample, and a flow meter, allowing for a 1-hour time integrated sample (see Turnbull et al., 2012 for full sampling system detail). This sampling regime prevents short time scale variations in mole fractions from biasing the sample (Turnbull et al., 2012).

2.2 Stable Isotope Analysis

The stable isotopic measurement procedure is described in detail in Vimont et al. (2017). Briefly, the air is extracted from the PFP by vacuum transfer through a cryogenic trap at -60° C that removes water vapor. Next, a mass flow controller is used to regulate the flow of the sample through a second cryogenic trap at -196° C that removes CO_2, N_2O, and any other condensable species. The remaining air is passed through acidified I_2O_5 suspended on a silica gel matrix (Schutze's reagent, Schutze, 1949) which quantitatively oxidizes CO to CO_2, adding O with a consistent isotopic signature. The sample passes through a second refrigerated loop trap to

Atmos. Chem. Phys. Discuss., https://doi.org/10.5194/acp-2018-506
Manuscript under review for journal Atmos. Chem. Phys.
Discussion started: 22 June 2018

remove any excess sulfuric acid that has evolved from the reagent, and finally the CO-derived CO_2 is trapped on a third cryogenic trap (also at -196° C) while the remaining gasses are pumped away. The CO-derived CO_2 is then transferred to a cryogenic focusing trap, and finally released through a GC column (PoraBond Q) to the isotope ratio mass spectrometer (GV Instruments IsoPrime 5KeV).

Following convention, we use delta notation to report our isotopic results:

$$\delta^{13}C_{VPDB} = \left(\frac{R_s}{R_{VPDB}} - 1\right) * 10^3‰ \qquad (1)$$

where R_s is the ratio of 13-carbon to 12-carbon in the sample, and R_{VPDB} is the ratio of 13-carbon to 12-carbon in the international standard Vienna Pee Dee Belemnite. The same relationship describes $\delta^{18}O$ except the international standard of reference is Vienna Standard Mean Ocean Water (VSMOW). Because we are oxidizing CO to CO_2 in this analysis, we must correct our CO_2 $\delta^{18}O$ data to account for the added oxygen, as described in Mak and Yang (1998):

$$\delta^{18}O_{CO} = 2\delta^{18}O_{CO_2} - \left(2\delta^{18}O_{CO_2 std} - \delta^{18}O_{COstd}\right) \qquad (2)$$

where the subscript CO indicates the original $\delta^{18}O$ signature of the sample, CO_2 indicates the $\delta^{18}O$ of the CO_2 measured in the mass spectrometer, CO_2std indicates the $\delta^{18}O$ of the CO_2 measured on the standard gas, and COstd indicates the calibrated $\delta^{18}O$ of the CO in the same standard gas (standard gas procedure was described in Vimont et al. (2017). Once the samples have been analyzed in the mass spectrometer, a correction for the ^{17}O contribution to the $\delta^{13}CO$ measurement is applied to the data based on the recommendations of Brand et al. (2009) (Vimont et al., 2017). This correction is required because ^{13}CO and $C^{17}O$ have the same mass and are indistinguishable in our mass spectrometer. The 1σ repeatability over two years for our analysis system is 0.23‰ for $\delta^{13}C$ and 0.46‰ for $\delta^{18}O$. For a more complete description of system performance, see Vimont et al. (2017).

We note that a significant deviation from the standard CO_2 ^{17}O correction has been observed and quantified for CO, particularly in the high northern latitudes (Röckmann and Brenninkmeijer, 1998; Röckmann et al., 1998). This so called "^{17}O

excess", or $\Delta^{17}O$, is a result of mass-independent fractionation (MIF) that arises in OH and O_3 photolytic formation (Röckmann et al., 1998; Huff and Thiemens, 1998). This effect can introduce error of up to 0.35‰ in the corrected $\delta^{13}C$ values, and is only quantifiable by measuring $\delta^{17}O$ (Röckmann and Brenninkmeijer, 1998). However, though we do not measure $\delta^{17}O$ for our samples, our analysis (section 2.5) precludes the need for this correction because both background and urban samples will see similar $\Delta^{17}O$ effects.

2.3 Simplification of the CO Budget

One of the advantages to the INFLUX experiment is the ability to remove background signals from the urban measurements, and thereby derive the urban enhancement. This approach also allows the CO budget to be simplified. Both the oxidation of CH_4 to CO and the oxidation of CO to CO_2 via the OH radical are reactions that proceed slowly relative to the experimental scale of a few hours transit time between the background and urban sites. Because of this, we calculate that these two processes have negligible impact on our urban CO enhancements, and can be disregarded given the short reaction time being considered.

The reaction time period can be calculated simply by considering the distance between tower 1 and towers 2 or 3 and the average wind speed. Given the average wind speed during sampling for this study was 4.4 ± 1.3 m s^{-1}, a 2.7-hour transit time is required. In this experiment, we correct our results to account for the incoming background CO and examine the urban contribution alone. This short transit time scale allows us to place constraints on the CH_4 oxidation source and the OH oxidation sink of CO.

Oxidation of CH_4 by OH is a major source of CO globally but CH_4 is long lived in the atmosphere relative to CO (Sander et al., 2006; Atkinson et al., 2006; Duncan et al., 2007). The approximate rate for the reaction of CH4 with OH is $6.4x10^{-15}$ cm^3 s^{-1} at

Atmos. Chem. Phys. Discuss., https://doi.org/10.5194/acp-2018-506
Manuscript under review for journal Atmos. Chem. Phys.
Discussion started: 22 June 2018

standard pressure and our mean ambient temperature of 26° C (Atkinson et al., 2006). OH mole fraction has been determined at urban sites in similar latitude bands and ranges from $1x10^6$ cm^{-3} in cool, winter time conditions to $2x10^7$ cm^{-3} in hot, summertime conditions (Warneke et al., 2007, 2013; Atkinson and Arey, 2003; Park et al., 2011). We do not have OH mole fraction measurements at Indianapolis, and therefore use the highest reported literature value for OH of $2x10^7$ cm^{-3} (Park et al., 2011) to assess the maximum CH_4 oxidation contribution to CO (Park et al., 2011, Table 2). We calculated the change in mole fraction of CO due to oxidation of CH_4 by OH by:

$$\Delta X_{CO} = \gamma(X_{CH_{4,i}})\left(1-e^{-k([OH])t}\right) \qquad (3)$$

where ΔX_{CO} is the change in CO mole fraction due to CH_4 oxidation by OH, γ is the CO yield for the CH_4+OH reaction (0.96 mole CO produced per mole CH_4), $X_{CH4,i}$ is the initial CH_4 mole fraction (the average CH_4 mole fraction during the sampling period, 1930 nmol:mol), k is the reaction rate for CH_4+OH ($6.4x10^{-15}$ cm^3 s^{-1}), [OH] is the high end member OH concentration from Park et al. (2011) ($2x10^7$ cm^{-3}, and t is the transit time of 2.7 hours.

We further assessed the impact on CO isotopes (Table 2) by using the reported isotopic values for CH_4 oxidation (Table 1). We calculated the change in $\delta^{13}C$ and $\delta^{18}O$ by

$$\Delta\delta = \delta_{CO,i} - \frac{(\delta_{CO,i}(X_{CO_i}))+\left(\delta_{CH_4}(X_{CO_{CH_4}})\right)}{\left(X_{CO_i}+X_{CO_{CH_4}}\right)} \qquad (4)$$

where Δδ is the change in either $\delta^{13}C$ or $\delta^{18}O$, δ_{COi} is the initial delta value at the polluted towers (average of the two towers (non-enhancement) of -29.6‰ for $\delta^{13}C$ and 5.1‰ for $\delta^{18}O$), X_{COi} is the CO mole fraction at the two polluted towers (average value of 166 nmol:mol), δ_{CH4} is the $\delta^{13}C$ or $\delta^{18}O$ value of CO produced by CH_4 oxidation (-52.6‰ and 0‰ for $\delta^{13}C$ and $\delta^{18}O$ respectively), and X_{COCH4} is the mole fraction of CO produced from oxidation of CH_4 by OH, calculated above.

Atmos. Chem. Phys. Discuss., https://doi.org/10.5194/acp-2018-506
Manuscript under review for journal Atmos. Chem. Phys.
Discussion started: 22 June 2018

Using these parameters and the average transit time between the towers of 2.7 hours, we calculate that during the transit across the city, CH_4 oxidation could contribute up to 1.4 nmol:mol CO, changing $\delta^{13}C$ by up to -0.21‰, and $\delta^{18}O$ by up to -0.04‰. These values are below our 1σ measurement uncertainties (0.23‰ $\delta^{13}C$ and 0.46‰ $\delta^{18}O$), and thus we do not consider CH_4 oxidation to be a significant source of CO in our analyses.

OH oxidation is the main sink of CO, and will directly impact the isotopic signatures of CO measured within the city (Röckmann and Brenninkmeijer, 1997; Duncan et al., 2007). Using the same method and OH mole fraction as for CH_4 oxidation above, and a reaction rate for CO+OH of 1.44×10^{-13} cm^3 s^{-1} (Atkinson et al., 2006), we calculated the net loss of CO during the transit of an air mass across the city. However, to calculate changes to the isotopic budget, we use the fractionation factors for OH oxidation found in Table 1 and a Rayleigh distillation approach to compute the impact of the OH sink on $\delta^{13}C$ and $\delta^{18}O$ of CO:

$$\frac{\delta_f}{10^3‰}+1=\left(\frac{\delta_i}{10^3‰}\right) f_f^{\alpha-1}+f_f^{\alpha-1} \qquad (5)$$

f refers to the final change in either $\delta^{13}C$ or $\delta^{18}O$, and i refers to the mean value of $\delta^{13}C$ or $\delta^{18}O$ measured at the two downwind towers (-29.9‰ for $\delta^{13}C$ and 4.1‰ for $\delta^{18}O$). f_f is the final fraction of CO left after the amount of CO lost is removed, determined by:

$$f_f=\frac{X_{CO_T}-X_{CO_{lost}}}{X_{CO_T}} \qquad (6)$$

where X_{COT} is the total CO mole fraction measured at tower 1 (mean value of 146 nmol:mol), and X_{COlost} is the amount of CO removed by oxidation with OH. α is the fractionation factor for either $\delta^{13}C$ or $\delta^{18}O$ from the literature (Table 1). The estimated total effect of OH oxidation on the CO mole fraction is 2.4 nmol:mol CO lost, -0.08‰ change in $\delta^{13}C$, and 0.17‰ change in $\delta^{18}O$. These changes in the isotopic values can also be neglected in our quantification of the CO isotopic budget given our estimated measurement uncertainty.

Biomass burning can be a source of CO in urban regions, though it is primarily used as a heat source (Saurer et al., 2009). Within Indianapolis, 2/3 of residential and commercial heating is done by natural gas combustion, and the remaining 1/3 is electrical (Gurney et al., 2012). Vimont et al. (2017) estimated that biomass burning for heat was only about 1% of the CO budget during the winter, and did not impact the isotopic budget significantly. As there should be much less (if any) biomass burning for heat during the summer, we assume that biomass burning is not a significant source of CO. Any biomass burning outside the city (burning off of crop fields or forest fires) is accounted for by removing the background.

The remaining sources of CO that must be considered are oxidation of VOC's (both biogenic and anthropogenic), and fossil fuel combustion. Fossil fuel combustion has long been considered the primary source of CO within urban regions (Stevens et al., 1972; EPA NEI 2011), whereas only recently has biogenic VOC oxidation been shown to be a significant urban source (Cheng et al., 2017).

2.4 Data filtering based on meteorological conditions

During the summer months, Indianapolis experiences thunderstorm activity, which is associated with convective air movement. When this convection occurs, it is possible the towers are influenced by air that is not representative of the urban enhancements due to entrainment of clean, free tropospheric air. Using data provided by NOAA's National Center for Environmental Information (NOAA NCEI), we obtained daily meteorological data for each sampling day (http://www.ncdc.noaa.gov/qclcd/QCLCD?prior=N). We removed days with winds that were calm, or had highly variable wind direction, as well as days with thunderstorm activity before, during, or directly after sampling occurred (Table 3). This filtering was necessary because these days with thunderstorms were also large outliers on our regression plots (figure 4). After removing these data, there were 16 (out of the initial 30) usable days for analysis.

Atmos. Chem. Phys. Discuss., https://doi.org/10.5194/acp-2018-506
Manuscript under review for journal Atmos. Chem. Phys.
Discussion started: 22 June 2018

Atmospheric Chemistry and Physics Discussions

2.5 Regression Plot Analysis

At Indianapolis the CO enhancements measured at towers 2 and 3 are small relative to the background CO at tower 1 (17 nmol:mol on average at tower 2, and 22 nmol:mol on average at tower 3 relative to average background CO at Tower 1 of 146 nmol:mol). Because of this, it is necessary to remove the background signal from the polluted towers to accurately constrain the urban signals. Using the method described by Miller and Tans (2003), we calculate the isotopic signature of the urban source:

$$\delta_s = \frac{\left(\delta_{meas} X_{CO_{meas}} - \delta_{bkg} X_{CO_{bkg}}\right)}{\left(X_{CO_{meas}} - X_{CO_{bkg}}\right)} \qquad (7)$$

where δ_s is the $\delta^{13}C$ or $\delta^{18}O$ of the urban source (Figure 4), the subscript meas indicates the $\delta^{13}C$ (or $\delta^{18}O$) and CO mole fraction measured at either tower 2 or 3. The subscript bkg indicates the $\delta^{13}C$ (or $\delta^{18}O$) and CO mole fraction measured at tower 1. We note that in equations (7) and (8) (below), the relationships hold only for the common mass isotopologue, but for small changes in the $^{13/12}C$ and $^{18/16}O$ ratios, the errors in these equations are negligible. In order to obtain a 'best-fit' solution using (3) for all the data, we regressed the numerator against the denominator using an ordinary least squares (model 1) Y|X approach, which assumes mole-fraction to be independent (Isobe et al.,1990; Zobitz et al., 2006).

To account for uncertainty in our measurements, we used a Monte Carlo technique. Using the propagated measurement uncertainties, we assigned an error distribution to each point. We assumed a normally distributed error curve based on QQ plot analysis (not shown). 10,000 regressions were run, randomly selecting values for each data point from that point's error distribution. The reported slopes are the median values from the 10,000 regressions. We use the median of the regression slopes rather than the mean because the median is more robust to outlier points than the mean (Miller et al., 2012). Because of the high scatter in our data set

Atmos. Chem. Phys. Discuss., https://doi.org/10.5194/acp-2018-506
Manuscript under review for journal Atmos. Chem. Phys.
Discussion started: 22 June 2018

(Figure 4), the median provides a better estimate of the overall δ_s in equation (7). The errors on the slope are 1σ for the slopes of each simulation. Finally, to assess how well our regression analysis results represent a solution for each point, we use the median slope and intercept to determine the residuals for each data point, and calculate an r^2 for each tower and isotope. r^2 is a metric for the strength of the correlation between x and y, and both uncertainty in the measured values and real atmospheric variability in the relationship between x and y will work to reduce r^2. Therefore, in this context, r^2 is a metric for determining the likelihood of a single source (or sources with identical isotopic signatures) or multiple sources with different isotopic signatures contributing to the CO signal on different days. High r^2 correspond to a single isotopic signature, whether by a single source or multiple sources, and a low r^2 corresponds to multiple isotopic source signatures varying through time.

2.6 Mass Balance Source Attribution

Through our calculations and reasoning above, we are able to neglect the CH_4 oxidation source, the biomass-burning source, and the OH oxidation sink. In order to constrain the remaining two sources (fossil fuel combustion and VOC oxidation, Duncan et al., 2007), we use a simple mass balance approach. We assume that the δ_s calculated at each polluted tower (section 2.5, equation (7)) can be represented by:

$$\delta_s = f_{VOC}\delta_{VOC} + f_{FF}\delta_{FF} \qquad (8a)$$

$$f_{VOC} + f_{FF} = 1 \qquad (8b)$$

where f_{VOC} and δ_{VOC} are the mole fraction and isotopic signature of VOC oxidation, and f_{FF} and δ_{FF} are the mole fraction and isotopic signature of fossil fuel combustion. The isotopic signatures of VOC oxidation are -32 ± 2‰ and 0 ± 3‰ for $\delta^{13}C$ and $\delta^{18}O$ respectively (Brenninkmeijer et al., 1999; Gros et al., 2001). These values have not been determined for this study area, and therefore have high uncertainty. The $\delta^{13}C$ and $\delta^{18}O$ values were originally determined by Stevens and Wagner (1989) by analyzing air in rural Illinois in the early 1970's. However, they did not account for

changing background air (via variable source distributions outside of their experimental area). Their approach assumed all CO added to the background was solely from VOC oxidation, but other sources may also have contributed. Further work by Brenninkmeijer (1993) and Röckmann and Brenninkmeijer (1997) suggest that the $\delta^{13}C$ value is reasonable, but assign ~2‰ uncertainty bounds (1σ). Conny et al. (1997) invoke a -3‰ fractionation factor for the oxidation of isoprene to CO, based on an average $\delta^{13}C$ of -29‰ for isoprene (Sharkey et al., 1991). However, Sharkey et al. (1991) suggest that the $\delta^{13}C$ may vary as plants are stressed, which is possible given the above mentioned urban heat island induced heat stress on urban trees (Califapietra et al., 2013). Moreover, they focused only on isoprene rather than a larger set of VOCs. From this perspective, the relatively large uncertainty suggested by Röckmann and Brenninkmeijer (1997) seems reasonable. Brenninkmeijer (1993) and Röckmann and Brenninkmeijer (1997) deduced a $\delta^{18}O$ value of 0‰ from their work in the high northern and southern latitudes. This value is generally accepted in the literature, yet disagrees substantially with Stevens and Wagner (1989), who calculated 15‰ from their study in rural Illinois. We use the value of 0 ±3‰ because it best explains the signals seen in several high latitude atmospheric studies (e.g. Röckmann et al., 2002; Park et al., 2015). We note that the uncertainty in these VOC isotopic signatures contribute a large portion of the overall uncertainty in the conclusions of this paper. More precise isotopic values for this oxidation process would drastically improve the estimates of VOC produced CO in isotope studies. The isotopic signatures of fossil fuel combustion at Indianapolis are -27.7 ± 0.5‰ and 17.7± 1.1‰ for $\delta^{13}C$ and $\delta^{18}O$ respectively (Vimont et al., 2017). Previously, we found that the isotopic signature in the winter did not vary with temperature significantly, and that the primary source within the city was emissions from transportation (Vimont et al., 2017). Therefore, we use these values as the fossil fuel produced CO isotopic signatures for Indianapolis. By solving (4a) and (4b) for f_{VOC} we are able to place a constraint on the VOC oxidation contribution to the urban CO budget.

Atmos. Chem. Phys. Discuss., https://doi.org/10.5194/acp-2018-506
Manuscript under review for journal Atmos. Chem. Phys.
Discussion started: 22 June 2018

3. Results and Discussion

3.1 Time Series

The full-time series of CO mole-fraction, $\delta^{13}C$, and $\delta^{18}O$ has been shown previously by Vimont et al. (2017) and figure 5 from that paper is reproduced here for completeness. Briefly, CO mole-fraction exhibits a seasonal trend that is similar to that found in other studies, with maximum CO occurring during the winter (February-March) and minimum values occurring in late summer (August) (Gros et al., 2001; Röckmann et al., 2002). Tower 2 and 3 are systematically enhanced relative to tower 1 (background), demonstrating consistent urban enhancement.

$\delta^{13}C$ and CO co-vary throughout the year, but lag behind $\delta^{18}O$ slightly. This trend in the mole fractions and the isotopes is similar to the results of Gros et al. (2001), who reported clean background air results from a mid-latitude site in Austria. However, this differs from the high latitude background signals reported by Röckmann et al. (2002). High latitude CO seasonal cycles are driven both by the OH sink and transport to and from the mid-latitudes (Röckmann et al., 2002), whereas mid-latitude continental sites have stronger influences from local or regional sources (Gros et al., 2001).

Towers 1 and 2 exhibit more negative isotopic signatures than tower 3 during the spring and summer months, likely due to higher fossil fuel contribution at the downtown location. The trend is consistent with VOC oxidation sources being more important at both tower 1 and 2. $\delta^{18}O$ shows a larger spread between all three towers relative to $\delta^{13}C$, which is also consistent with the larger difference in $\delta^{18}O$ between the fossil fuel combustion and VOC oxidation sources.

3.2 Partitioning fossil fuel combustion and VOC oxidation in the summertime urban CO budget

Atmos. Chem. Phys. Discuss., https://doi.org/10.5194/acp-2018-506
Manuscript under review for journal Atmos. Chem. Phys.
Discussion started: 22 June 2018

Atmospheric Chemistry and Physics Discussions

The Monte Carlo regression analysis produced urban source isotopic results of -28.8 ± 2.3‰ and -27.7 ± 2.1‰ for $\delta^{13}C$, and 10.9 ± 3.2‰ and 13.0 ±4.9‰ for $\delta^{18}O$ at towers 2 and 3 respectively (Figure 4). In both isotopes, tower 2 is associated with lower urban source isotopic values than tower 3. With the higher variability in $\delta^{18}O$ measurements than the $\delta^{13}C$, the r^2 was lower ($r^2 > 0.9$ for $\delta^{13}C$, $r^2 \sim 0.4$ for $\delta^{18}O$)(Figure 4). The $\delta^{13}C$ source signature is not significantly different from summer to winter (-27.7±0.5‰ in winter, Vimont et al., 2017), which is reasonable since the VOC derived CO isotopic signature (-32±2‰) is relatively close to the Indianapolis fossil fuel combustion $\delta^{13}C$ isotopic signature. However, the $\delta^{18}O$ signature is substantially lighter in summer than in winter (17.7±1.0‰ in winter, Vimont et al., 2017). These results are consistent with a VOC oxidization source in the summer.

We note that the isotopic data show greater scatter in our regression plots (r^2~0.9 and 0.4 for $\delta^{13}C$ and $\delta^{18}O$ respectively, Figure 4) than was observed for the wintertime (r^2~0.98 and 0.88 for $\delta^{13}C$ and $\delta^{18}O$ respectively) when the CO enhancement is driven almost exclusively by fossil fuel emissions (Vimont et al., 2017). This additional variability can be explained by varying contributions of VOC oxidation from day to day, affecting the fractional contribution of VOC oxidation and fossil fuel combustion to the overall urban CO enhancement. For example, isoprene oxidation is a highly variable source of CO because isoprene emissions depend exponentially on the ambient temperature, and the rate at which isoprene is oxidized will increase as NO_x increases (Guenther et al., 1995; Carter and Atkinson, 1996). Both the temperature and boundary layer mixing will vary day to day. Differences in the $\delta^{18}O$ signatures of the fossil and VOC oxidation sources are much greater than differences in the respective $\delta^{13}C$ signatures, which drive the observed increased scatter in the $\delta^{18}O$ regression data.

Atmos. Chem. Phys. Discuss., https://doi.org/10.5194/acp-2018-506
Manuscript under review for journal Atmos. Chem. Phys.
Discussion started: 22 June 2018

Atmospheric Chemistry and Physics Discussions

Using the mass balance approach described in section 2.5, we calculated the contribution to urban CO enhancements arising from oxidized VOC's during the summer months to be 38 ± 20% at tower 2, and 27±29% (1σ) at tower 3, resulting in a VOC source contribution range of 0-58% of the urban enhancements during the summer. The remainder of the CO enhancement (40-100%) is due to fossil fuel combustion. The variability in the determined VOC contributions is likely due in large part to the variable emission of BVOC's (discussed above), but this is not apparent in our small dataset

For this calculation, we only considered the $\delta^{18}O$ signatures at each tower. Due to the small difference in $\delta^{13}C$ between fossil fuel combustion and VOC oxidation (-27.7±0.5‰ vs. -32±2‰) and the relatively large uncertainties in the δ_s signatures calculated from our regression analysis, no meaningful source attribution is possible with our mass balance approach. However, the shift we see in $\delta^{13}C$ at tower 2 is qualitatively consistent with an increased VOC oxidation source (figure 4).

Tower 2 exhibits lighter $\delta^{18}O$ than tower 3 on average, implying a larger contribution of VOC oxidized CO at this site than at tower 3. The distance between towers 1 and 2 is larger than the distance between towers 1 and 3, which allows more time for oxidation reactions to occur. Further, the footprint of tower 2 contains more biogenic sources than tower 3 (section 2.1; Turnbull et al., 2015), which is also consistent with an increased VOC oxidation source at tower 2.

3.3 Possible Urban VOC Sources

The most likely sources of the oxidized VOC's present in this study are biogenically produced isoprene, methanol, and monoterpenes. BVOC's are primarily produced from deciduous and coniferous trees. These emissions exceed anthropogenic VOC emissions globally by a factor of four (Lamb et al., 1987; Guenther et al., 1991; Warneke et al., 2010). Isoprene is produced from deciduous trees during the spring

and summer growing season, and its emissions are estimated to comprise 50-60% of the BVOC budget, (Guenther et al., 1993, 1995; Helmig et al., 1998; Harley et al., 1999). The emission of isoprene increases exponentially with temperature (Guenther et al., 1995). Within urban environments, temperatures are amplified by the urban heat island effect, therefore subjecting urban trees to higher temperatures than rural trees (Oke, 1973; Takebayashi and Moriyama, 2009; Califapietra et al., 2013). Concrete and asphalt can reach temperatures of 60° C, re-radiating heat into the urban atmosphere and raising the air temperature by 5-10° C (calculated) relative to the same location were the city not present (Oke, 1973; Takebayashi and Moriyama, 2009). It is thought that isoprene emission is due to heat stress (Califapietra et al., 2013).

Once isoprene has been emitted, it is rapidly destroyed through reactions with OH and ozone (O_3) (Carter and Atkinson, 1996). Within polluted regions such as cities, increased OH and O_3 levels result in a 30-60 minute lifetime for isoprene (Warneke et al., 2010). This lifetime is short compared to what is estimated from unpolluted forest, using the global average OH mole fraction ($1x10^6$ cm^{-3}) and the reaction rate of isoprene with OH ($3.1x10^{-11}$ cm^3 sec^{-1}) (Atkinson et al., 2006) which is about 3 hours. CO is not a direct product of isoprene in the atmosphere (Carter and Atkinson 1996). Isoprene oxidizes to products such as formaldehyde, methacrolien (MACR), and methyl-vinyl-keytone (MVK), which are rapidly oxidized by OH, O_3, or *hv* to form CO (Carter and Atkinson, 1996). The resultant yield of CO from isoprene oxidation (n molecules CO:1 molecule isoprene) ranges from 1:2 in NO_x depleted conditions to 3.2:1 in high NO_x conditions (Miyoshi et al., 1994; Holloway et al., 2000; Duncan et al., 2007; Grant et al., 2010).

The other main CO-producing BVOC's are methanol, monoterpenes, and acetone. (Duncan et al., 2007). Methanol is the second largest BVOC source of CO globally, followed by monoterpenes such as α and β pinene, and lastly acetone (Duncan et al., 2007). Monoterpenes, like isoprene, have short lifetimes in the atmosphere, ranging

from around a minute (α-terpenine + O_3/NO_3) to over a day (β-pinene + O_3) (Atkinson and Arey, 2003). However, methanol and acetone have much longer lifetimes than isoprene: 12 days (methanol + OH) and 61 days (acetone +OH) (Atkinson and Arey, 2003).

Anthropogenic volatile organic compounds (AVOC's) are also a source of CO via oxidation reactions, and in urban regions, AVOC emissions can be a larger source of VOCs than BVOC emissions (Atkinson and Arey, 2003; Borbon et al., 2013; Ammoura et al., 2014). Further, isoprene, MVK, MACR, methanol and acetone all have minor anthropogenic sources (relative to their biogenic sources), the most prominent being automobile exhaust (Biesenthal et al., 1997; Cheung et al., 2014). AVOC emissions are less variable than BVOC emissions throughout the year, but some, such as evaporative emissions from gasoline processes, increase during the summer (Jordan et al., 2009). Therefore, their contribution to the CO budget must be considered.

However, biogenic and anthropogenic VOC sources cannot currently be separated using stable isotopes. Only a combined isotopic signature has been estimated for VOC oxidation to CO, and CO isotopic signatures associated with specific VOC oxidation pathways have not yet been quantified. Therefore, we have assessed the likely CO yields from the most prevalent VOC compounds using estimated abundances and reaction kinetics (Table 4).

While BVOC emissions dominate globally, AVOC emissions are important in urban regions, specifically for O_3 and secondary organic aerosol prediction modeling (Warneke et al., 2007; Bourbon et al., 2013, references therein). As with BVOC emissions, AVOC emissions increase in the summer months; however, AVOC's are present year round, with smaller seasonal variations than BVOC's (Jordan et al., 2009). Several compounds, such as isoprene and methanol, have both biogenic and anthropogenic sources, though for both isoprene and methanol, the biogenic source is much larger than the anthropogenic source (Singh et al., 2000; Jordan et al., 2009;

Wagner et al., 2014). Further, in the late 1980's, Chameides et al. (1988) showed that BVOC's were of equal or greater importance than AVOC's in Atlanta, GA. As emission controls have steadily improved over the last three decades, there has been a continual reduction in urban AVOC emissions (Dollard et al., 2007; von Schneidemesser et al., 2010; Wagner et al., 2014). The INFLUX sampling regime (section 2.1) provides only 2.7 hours (on average) for oxidation reactions to produce CO, and thus only the fastest reacting VOC's will contribute to the urban enhancements (Table 4). Though AVOC mole-fractions are often elevated relative to BVOC's in urban regions, very few have short enough lifetimes to produce significant amounts of CO in this experiment (Table 4, Atkinson and Arey, 2003; Jordan et al., 2009; Warneke et al., 2013).

In addition to being highly reactive, a VOC must be present in high enough mole fraction to significantly impact the CO budget. Jordan et al. (2009) produced a long-term time series from rural New Hampshire for many common anthropogenic and biogenic VOC's. Of those species measured, the highest summer time mole fractions were seen in isoprene (and its immediate products, methyl-vinyl keytone (MVK) and macroelien (MACR)), monoterpenes, methanol, and acetone (Table 4, Jordan et al., 2009). The largest mole fractions are seen midday to mid afternoon (Karl et al., 2003; Jordan et al., 2009; Park et al., 2011; Wagner et al., 2014). Karl et al. (2003) and Park et al., (2011) observed maximum, midday isoprene mole fractions of 26 nmol:mol in La Porte and Houston, Texas, USA. Granier et al. (2000) used the IMAGES 3D Chemistry Transport Model to simulate isoprene emissions, and found a mean July isoprene mole fraction of 1 nmol:mol over Indianapolis. This agrees well with the median (four summers) summertime value of approximately 0.75 nmol:mol found for isoprene + MVK and MACR found by Jordan et al. (2009). Because the isotopic signatures of our urban enhancements are calculated using data over the entire summer, we chose to use the summertime mole-fraction measurements determined by Jordan et al. (2009) for isoprene + MVK and MACR, monoterpenes, methanol, toluene, acetone, and benzene. For the remaining

compounds, we approximated the mole fractions using the VOC:CO emission ratios from Warneke et al. (2013).

Lastly, the chemical yield of each reaction must be considered. In the case of isoprene, under high NOx conditions (such as those found in urban environments), the CO yield from isoprene is 3.05:1 (61% carbon) (Grant et al., 2010)(Table 4). Therefore, not only is isoprene oxidized rapidly, but also each oxidized isoprene molecule may produce three molecules of CO. Methanol has a chemical yield of 0.98:1 (98% carbon), and therefore produces one CO molecule per methanol molecule oxidized.

In order to assess the overall impact of various VOC's on the CO budget, we used mole-fraction measurements (where available) and / or emission ratio estimates to approximate the VOC budget for 20 of the most abundant biogenic and anthropogenic VOC's (Table 4). We then calculated the net loss of each VOC based on their OH, O_3, and NO_3 reactivities (Atkinson et al., 2006; Sander et al., 2006) (Table 4). In order to assess the maximum yield, we used high-end values of OH, O_3, and NO_3 mole fractions found in the literature. We took a value of $2x10^7$ cm^{-3} for the OH mole fraction found in Park et al. (2011). Both the O_3 mole fraction ($7x10^{11}$ cm^{-3}) and the NO_3 mole fraction ($2.5x10^8$ cm^{-3}) were taken from Atkinson and Arey (2003). Finally, we applied the chemical yield for the VOC's to CO (Altshuller, 1991; Grant et al., 2010).

Through these calculations, we determined that isoprene, methanol, monoterpenes, toluene and ethene oxidation could be significant in the CO budget, adding 6.2 nmol:mol of CO to the urban enhancement (Table 4) during the 2.7 hour transit time. This result is in good agreement with the VOC produced CO estimates from our isotopic analysis. Using the average CO enhancement for towers 2 and 3 (19.5 nmol:mol), the predicted VOC oxidation contribution from our isotopic analysis is 6.3 nmol:mol (section 3.1). These calculations were done using high mole fraction estimates for the various oxidants, suggesting that these oxidants may be present at

high mole fractions in Indianapolis. Finally, isoprene, methanol, and the monoterpenes are primarily produced biogenically, suggesting that biogenic VOC oxidation likely dominates the VOC derived CO budget in the summer at Indianapolis.

3.4 Declining Anthropogenic Emissions

Anthropogenic emissions of CO and VOCs in the United States and Europe have been declining for several decades due to emission control campaigns (e.g. Bishop and Stedmann, 2008; Bourbon et al., 2013). For CO, anthropogenic emissions still dominate the overall urban budget, as evidenced by this study, as well as others (e.g. EPA NEI 2011; Turnbull et al., 2015; Vimont et al., 2017). However, as early as the late 1980's, urban studies of VOCs showed that biogenic VOCs could be a significant portion of the urban VOC budget (e.g. Chameides et al., 1988). Chameides et al. (1988) also note that fast reacting biogenic VOC's, such as isoprene, can have a greater impact on species produced through oxidation effects. These include O_3 and CO, and thus BVOC's can contribute more strongly to the urban CO budget than anthropogenic VOC's. It is possible that urban planning has increased the number of trees within cities, although we do not have direct evidence to support this at Indianapolis. Cheng et al. (2017) found that the CO budget in the Washington DC area was similarly dominated by anthropogenic CO emissions and oxidation of isoprene, with near equal contributions. They used a modeling approach comparing O_3 and CO (using O_3 and CO observations), a method independent of our own. They also attribute this increased influence of isoprene oxidation to the gradual decrease in anthropogenic emissions, largely in the mobile sector (Cheng et al., 2017). We find that fossil emissions most likely still dominate the Indianapolis summertime CO budget. However, VOC oxidation sources can exceed anthropogenic emissions within our 1σ uncertainty, which is consistent with Cheng et al. (2017).

4. Conclusions

Our CO isotope results from Indianapolis provide the strongest empirical evidence to date that VOC oxidation represents a major source of CO in summertime urban environments. The determined contribution of VOC oxidation to the total urban CO source ranged from 0 to 58% (1σ range) depending on date and location with the remainder (42-100%) from fossil fuel combustion. While we were unable to confirm the VOC source directly, oxidation of VOC's to CO in conjunction with fossil fuel emissions provides the most plausible explanation for our isotopic results.

Estimates of the likely mole fractions of different VOC's and their respective reactivities suggests that biogenic VOC's (primarily isoprene, methanol, and monoterpenes) rather than anthropogenic VOCs are likely responsible for the majority of the VOC-produced CO. Throughout the year, fossil fuel emissions still dominate the urban budget. However, our study makes it apparent that during the summer, the VOC oxidation source can be of similar magnitude to the fossil fuel combustion source in an urban area and therefore must be considered as important during the growing season in future urban CO inventories and studies. Finally, the uncertainties highlighted in much of this study, particularly with respect to the oxidized VOC isotopic signatures, underscore the need for continued research into CO stable isotopes, and the isotopic signatures of the CO sources.

Author contributions:

IJV performed the measurements, data analysis, and wrote the article. JCT assisted in data analysis and provided multiple coauthor revisions. VVP provided assistance with measurement issues, data analysis, and multiple coauthor revisions. PFP assisted in several of the measurements. CS provided several coauthor revisions. NM and SR provided logistical support for sample collection for the measurements. BHV and JWCW provided laboratory and equipment support.

Competing Financial Interests:

There are no competing financial interests for any of the authors.

Funding Sources:

This research was generously funded by the National Institute of Standards and Technology (grant 60NANB10D023) and the National Oceanic and Atmospheric Administration Climate Program Office's AC4 program (award NA13OAR4310074). The lead author and the analysis system development were supported through funding in conjunction with the INSTAAR contract for isotopic analysis (RA-133R-15-CQ-0044) with The National Oceanic and Atmospheric Administration (NOAA) Earth System Research Laboratory (ESRL) Global Monitoring Division (GMD) Global Greenhouse Gas Reference Network (GGGRN).

Materials and Correspondence:

Please direct all requests for materials and correspondence to Isaac J Vimont, Isaac.vimont@colorado.edu

Data Availability:

Data for this experiment is available in Table 5, included in this manuscript.

References

Altshuller, A. P. (1991), The production of carbon-monoxide by the homogeneous nox-induced photooxidation of volatile organic-compounds in the troposphere, *Journal of Atmospheric Chemistry*, *13*(2), 155-182, doi:10.1007/bf00115971.

Ammoura, L., I. Xueref-Remy, V. Gros, A. Baudic, B. Bonsang, J. E. Petit, O. Perrussel, N. Bonnaire, J. Sciare, and F. Chevallier (2014), Atmospheric measurements of ratios between CO2 and co-emitted species from traffic: a tunnel study in the Paris megacity, *Atmospheric Chemistry and Physics*, *14*(23), 12871-12882, doi:10.5194/acp-14-12871-2014.

Atkinson, R., and J. Arey (2003), Gas-phase tropospheric chemistry of biogenic volatile organic compounds: a review, *Atmospheric Environment*, *37, Supplement 2*, 197-219, doi:http://dx.doi.org/10.1016/S1352-2310(03)00391-1.

Atkinson, R., D. L. Baulch, R. A. Cox, J. N. Crowley, R. F. Hampson, R. G. Hynes, M. E. Jenkin, M. J. Rossi, and J. Troe (2006), Evaluated kinetic and photochemical data for atmospheric chemistry: Volume II - gas phase reactions of organic species, *Atmospheric Chemistry and Physics*, *6*, 3625-4055

Biesenthal, T. A., Q. Wu, P. B. Shepson, H. A. Wiebe, K. G. Anlauf, and G. I. Mackay (1997), A study of relationships between isoprene, its oxidation products, and ozone, in the Lower Fraser Valley, BC, *Atmospheric Environment*, *31*(14), 2049-2058, doi:10.1016/s1352-2310(96)00318-4.

Bishop, G. A., and D. H. Stedman (2008), A decade of on-road emissions measurements, *Environ. Sci. Technol.*, *42*(5), 1651-1656, doi:10.1021/es702413b.

Borbon, A., et al. (2013), Emission ratios of anthropogenic volatile organic compounds in northern mid-latitude megacities: Observations versus emission inventories in Los Angeles and Paris, *J. Geophys. Res.-Atmos.*, *118*(4), 2041-2057, doi:10.1002/jgrd.50059.

Brand, W. A., S. S. Assonov, and T. B. Coplen (2009), Correction for the 17O Interference in d13C Measurements When Analyzing CO2 with Stable Isotope Mass Spectrometry*Rep.*, International Union of Pure and Applied Chemistry Inorganic Chemistry Division Commission on Isotopic Abundances and Atomic Weights.

Brenninkmeijer, C. A. M. (1993), Measurement of the Abundance of 14CO in the Atmosphere and the 13C/12C and 18O/16O Ratio of Atmospheric CO with Applications in New Zealand and Antarctica, *Journal of Geophysical Research*, *98*(D6), 10,595-510,614.

Brenninkmeijer, C. A. M., T. Röckmann, M. Braunlich, P. Jockel, and P. Bergamaschi (1999), Review of Progress in Isotope Sutdies of Atmospheric Carbon Monoxide, *ChemoSphere- Global Change Science*, *1*, 33-52.

Calfapietra, C., S. Fares, F. Manes, A. Morani, G. Sgrigna, and F. Loreto (2013), Role of Biogenic Volatile Organic Compounds (BVOC) emitted by urban trees on ozone concentration in cities: A review, *Environ. Pollut.*, *183*, 71-80, doi:10.1016/j.envpol.2013.03.012.

Carter, W. P. L., and R. Atkinson (1996), Development and evaluation of a detailed mechanism for the atmospheric reactions of isoprene and NOx, *Int. J. Chem. Kinet.*, *28*(7), 497-530, doi:10.1002/(sici)1097-4601(1996)28:7<497::aid-kin4>3.0.co;2-q.

Chameides, W. L., R. W. Lindsay, J. Richardson, and C. S. Kiang (1988), The role of biogenic hydrocarbons in urban photochemical smog - atlanta as a case-study, *Science*, *241*(4872), 1473-1475, doi:10.1126/science.3420404.

Cheng, Y., Y. H. Wang, Y. Z. Zhang, G. Chen, J. H. Crawford, M. M. Kleb, G. S. Diskin, and A. J. Weinheimer (2017), Large biogenic contribution to boundary layer O-3-CO regression slope in summer, *Geophysical Research Letters*, *44*(13), 7061-7068, doi:10.1002/2017gl074405.

Cheung, K., H. Guo, J. M. Ou, I. J. Simpson, B. Barletta, S. Meinardi, and D. R. Blake (2014), Diurnal profiles of isoprene, methacrolein and methyl vinyl ketone at an urban site in Hong Kong, *Atmospheric Environment*, *84*, 323-331, doi:10.1016/j.atmosenv.2013.11.056.

Conny, J. M., R. M. Verkouteren, and L. A. Currie (1997), Carbon 13 composition of tropospheric CO in Brazil: A model scenario during the biomass burn season, *J. Geophys. Res.-Atmos.*, *102*(D9), 10683-10693, doi:10.1029/97jd00407

Dollard, G. J., P. Dumitrean, S. Telling, J. Dixon, and R. G. Derwent (2007), Observed trends in ambient concentrations of C-2-C-8 hydrocarbons in the United Kingdom over the period from 1993 to 2004, *Atmospheric Environment*, *41*(12), 2559-2569, doi:10.1016/j.atmosenv.2006.11.020.

Duncan, B. N., J. A. Logan, I. Bey, I. A. Megretskaia, R. M. Yantosca, P. C. Novelli, N. B. Jones, and C. P. Rinsland (2007), Global budget of CO, 1988–1997: Source estimates and validation with a global model, *Journal of Geophysical Research: Atmospheres*, *112*(D22), D22301, doi:10.1029/2007jd008459.

Granier, C., G. Petron, J. F. Muller, and G. Brasseur (2000), The impact of natural and anthropogenic hydrocarbons on the tropospheric budget of carbon monoxide, *Atmospheric Environment*, *34*(29-30), 5255-5270, doi:10.1016/s1352-2310(00)00299-5.

Grant, A., A. T. Archibald, M. C. Cooke, and D. E. Shallcross (2010), Modelling the oxidation of seventeen volatile organic compounds to track yields of CO and CO2, *Atmospheric Environment*, *44*(31), 3797-3804, doi:10.1016/j.atmosenv.2010.06.049.

Griffin, R. J., J. J. Chen, K. Carmody, S. Vutukuru, and D. Dabdub (2007), Contribution of gas phase oxidation of volatile organic compounds to atmospheric carbon monoxide levels in two areas of the United States, *J. Geophys. Res.-Atmos.*, *112*(D10), 19, doi:10.1029/2006jd007602.

Gros, V., et al. (2001), Detailed analysis of the isotopic composition of CO and characterization of the air masses arriving at Mount Sonnblick (Austrian Alps), *Journal of Geophysical Research*, *106*(D3), 3179-3193.

Gros, V., P. Jöckel, C. Brenninkmeijer, T. Röckmann, F. Meinhardt, and R. Graul (2002), Characterization of pollution events observed at Schauinsland, Germany, using CO and its stable isotopes, *Atmospheric environment*, *36*(17), 2831-2840.

Guenther, A., et al. (1995), A global-model of natural volatile organic-compound emissions, *J. Geophys. Res.-Atmos.*, *100*(D5), 8873-8892, doi:10.1029/94jd02950.

Guenther, A. B., R. K. Monson, and R. Fall (1991), Isoprene and monoterpene emission rate variability - observations with eucalyptus and emission rate algorithm development, *J. Geophys. Res.-Atmos.*, *96*(D6), 10799-10808, doi:10.1029/91jd00960.

Guenther, A. B., P. R. Zimmerman, P. C. Harley, R. K. Monson, and R. Fall (1993), Isoprene and monoterpene emission rate variability - model evaluations and sensitivity analyses, *J. Geophys. Res.-Atmos.*, *98*(D7), 12609-12617, doi:10.1029/93jd00527.

Gurney, K. R., I. Razlivanov, Y. Song, Y. Y. Zhou, B. Benes, and M. Abdul-Massih (2012), Quantification of Fossil Fuel CO2 Emissions on the Building/Street Scale for a Large US City, *Environ. Sci. Technol.*, *46*(21), 12194-12202, doi:10.1021/es3011282.

Harley, C. P., K. R. Monson, and T. M. Lerdau (1999), Ecological and evolutionary aspects of isoprene emission from plants, *Oecologia*, *118*(2), 109-123, doi:10.1007/s004420050709.

Helmig, D., J. Greenberg, A. Guenther, P. Zimmerman, and C. Geron (1998), Volatile organic compounds and isoprene oxidation products at a temperate deciduous forest site, *J. Geophys. Res.-Atmos.*, *103*(D17), 22397-22414, doi:10.1029/98jd00969.

Holloway, T., H. Levy, and P. Kasibhatla (2000), Global distribution of carbon monoxide, *J. Geophys. Res.-Atmos.*, *105*(D10), 12123-12147, doi:10.1029/1999jd901173.

Huff, A. K., and M. H. Thiemens (1998), O-17/O-16 and O-18/O-16 isotope measurements of atmospheric carbon monoxide and its sources, *Geophysical Research Letters*, *25*(18), 3509-3512, doi:10.1029/98gl02603.

Isobe, T., E. D. Feigelson, M. G. Akritas, and G. J. Babu (1990), Linear-regression in astronomy .1, *Astrophys. J.*, *364*(1), 104-113, doi:10.1086/169390.

Jordan, C., E. Fitz, T. Hagan, B. Sive, E. Frinak, K. Haase, L. Cottrell, S. Buckley, and R. Talbot (2009), Long-term study of VOCs measured with PTR-MS at a rural site in New Hampshire with urban influences, *Atmospheric Chemistry and Physics*, *9*(14), 4677-4697.

Kanakidou, M., and P. J. Crutzen (1999), The photochemical source of carbon monoxide: Importance, uncertainties and feedbacks, *Chemosphere - Global Change Science*, *1*(1-3), 91-109.

Karl, T., T. Jobson, W. C. Kuster, E. Williams, J. Stutz, R. Shetter, S. R. Hall, P. Goldan, F. Fehsenfeld, and W. Lindinger (2003), Use of proton-transfer-reaction mass spectrometry to characterize volatile organic compound sources at the La Porte super site during the Texas Air Quality Study 2000, *J. Geophys. Res.-Atmos.*, *108*(D16), 15, doi:10.1029/2002jd003333.

Kato, S., H. Akimoto, M. Braunlich, T. Röckmann, and C. A. M. Brenninkmeijer (1999), Measurements of stable carbon and oxygen isotopic compositions of CO in automobile exhausts and ambient air from semi-urban Mainz, Germany, *Geochem. J.*, *33*(2), 73-77.

Lamb, B., A. Guenther, D. Gay, and H. Westberg (1987), A national inventory of biogenic hydrocarbon emissions, *Atmospheric Environment*, *21*(8), 1695-1705, doi:10.1016/0004-6981(87)90108-9.

Logan, J. A., M. J. Prather, S. C. Wopsy, and M. B. McElroy (1981), Tropospheric Chemistry: A Global Perspective, *Journal of Geophysical Research*, *86*(C8), 7210-7254.

Mak, J. E., and G. Kra (1999), The isotopic composition of carbon monoxide at Montauk Point, Long Island, *ChemoSphere- Global Change Science*, *1*, 205-218.

Mak, J. E., and W. Yang (1998), Technique for Analysis of Air Samples for 13C and 18O in Carbon Monoxide via Continuous-Flow Isotope Ratio Mass Spectrometry, *Analyitical Chemistry*, *70*, 5159-5161.

Miles, N. L., et al. (2017), Quantification of urban atmospheric boundary layer greenhouse gas dry mole fraction enhancements in the dormant season: Results

from the Indianapolis Flux Experiment (INFLUX), *Elem Sci Anth*, *5*(27), doi:http://doi.org/10.1525/elementa.127.

Miller, J. B., et al. (2012), Linking emissions of fossil fuel CO2 and other anthropogenic trace gases using atmospheric (CO2)-C-14, *J. Geophys. Res.-Atmos.*, *117*, 23, doi:10.1029/2011jd017048.

Miller, J. B., and P. P. Tans (2003), Calculating isotopic fractionation from atmospheric measurements at various scales, *Tellus Ser. B-Chem. Phys. Meteorol.*, *55*(2), 207-214, doi:10.1034/j.1600-0889.2003.00020.x.

Miyoshi, A., S. Hatakeyama, and N. Washida (1994), OM radical-initiated photooxidation of isoprene - an estimate of global co production, *J. Geophys. Res.-Atmos.*, *99*(D9), 18779-18787, doi:10.1029/94jd01334.

Novelli, P. C., K. A. Masarie, P. M. Lang, B. D. Hall, R. C. Myers, and J. W. Elkins (2003), Reanalysis of tropospheric CO trends: Effects of the 1997-1998 wildfires, *J. Geophys. Res.-Atmos.*, *108*(D15), 14, doi:10.1029/2002jd003031.

Oke, T. R. (1973), City size and urban heat island, *Atmospheric Environment*, *7*(8), 769-779, doi:10.1016/0004-6981(73)90140-6.

Park, C., G. W. Schade, and I. Boedeker (2011), Characteristics of the flux of isoprene and its oxidation products in an urban area, *J. Geophys. Res.-Atmos.*, *116*, 13, doi:10.1029/2011jd015856.

Park, K., Z. H. Wang, L. K. Emmons, and J. E. Mak (2015), Variation of atmospheric CO, delta C-13, and delta O-18 at high northern latitude during 2004-2009: Observations and model simulations, *J. Geophys. Res.-Atmos.*, *120*(20), 13, doi:10.1002/2015jd023191.

Popa, M. E., M. K. Vollmer, A. Jordan, W. A. Brand, S. L. Pathirana, M. Rothe, and T. Röckmann (2014), Vehicle emissions of greenhouse gases and related tracers from a tunnel study: CO: CO2, N2O: CO2, CH4 : CO2, O-2 : CO2 ratios, and the stable isotopes C-13 and O-18 in CO2 and CO, *Atmospheric Chemistry and Physics*, *14*(4), 2105-2123, doi:10.5194/acp-14-2105-2014.

Röckmann, T., and C. A. M. Brenninkmeijer (1997), CO and CO2 isotopic composition in Spitsbergen during the 1995 ARCTOC campaign, *Tellus*, *49B*, 455-465.

Röckmann, T., and C. A. M. Brenninkmeijer (1998), The error in conventionally reported 13C/12C ratios of atmospheric CO due to the presence of mass independent oxygen isotope enrichment, *Geophysical Research Letters*, *25*(16), 3163-3166.

Röckmann, T., C. A. M. Brenninkmeijer, G. Saueressig, P. Bergamaschi, J. N. Crowley,

H. Fischer, and P. J. Crutzen (1998), Mass-Independent Oxygen Isotope Fractionation in Atmospheric CO as a Result of the Reaction CO+OH, *Science*, *281*(5376), 544-546, doi:10.1126/science.281.5376.544.

Röckmann, T., P. Jockel, V. Gros, M. Braunlich, G. Possnert, and C. A. M. Brenninkmeijer (2002), Using 14C, 13C, 18O, and 17O isotopic variations to provide insights into the high northern latitude surface CO inventory, *Atmospheric Chemistry and Physics*, *2*, 147-159.

Sakugawa, H., and I. R. Kaplan (1997), Radio- and stable-isotope measurements of atmospheric carbon monoxide in Los Angeles, *Geochem. J.*, *31*(2), 75-83.

Sander, S. P., R. Friedl, D. Golden, M. Kurylo, G. Moortgat, H. Keller-Rudek, P. Wine, A. Ravishankara, C. Kolb, and M. Molina (2006), *Chemical kinetics and photochemical data for use in atmospheric studies: evaluation number 15*, National Aeronautics and Space Administration, Jet Propulsion Laboratory, California Institute of Technology Pasadena, CA.

Saurer, M., A. S. H. Prevot, J. Dommen, J. Sandradewi, U. Baltensperger, and R. T. W. Siegwolf (2009), The influence of traffic and wood combustion on the stable isotopic composition of carbon monoxide, *Atmospheric Chemistry and Physics*, *9*, 3147-3161.

Sharkey, T. D., F. Loreto, C. F. Delwiche, and I. W. Treichel (1991), Fractionation of carbon isotopes during biogenesis of atmospheric isoprene, *Plant Physiol.*, *97*(1), 463-466, doi:10.1104/pp.97.1.463.

Singh, H., et al. (2000), Distribution and fate of selected oxygenated organic species in the troposphere and lower stratosphere over the Atlantic, *J. Geophys. Res.-Atmos.*, *105*(D3), 3795-3805, doi:10.1029/1999jd900779.

Stevens, C. M., L. Krout, D. Walling, and A. Venters (1972), The Isotopic Composition of Atmospheric Carbon Monoxide, *Earth and Planetary Science Letters*, *16*, 147-165.

Stevens, C. M., and A. F. Wagner (1989), The role of isotope fractionation effects in atmospheric chemistry, *Z. Naturfors. Sect. A-J. Phys. Sci.*, *44*(5), 376-384.

Takebayashi, H., and M. Moriyama (2009), Study on the urban heat island mitigation effect achieved by converting to grass-covered parking, *Sol. Energy*, *83*(8), 1211-1223, doi:10.1016/j.solener.2009.01.019.

Tsunogai, U., Y. Hachisu, D. D. Komatsu, F. Nakagawa, T. Gamo, and K.-i. Akiyama (2003), An updated estimation of the stable carbon and oxygen isotopic compositions of automobile CO emissions, *Atmospheric Environment*, *37*(35), 4901-4910, doi:10.1016/j.atmosenv.2003.08.008.

Turnbull, J., D. Guenther, A. Karion, C. Sweeney, E. Anderson, A. Andrews, J. Kofler, N. Miles, T. Newberger, and S. Richardson (2012), An integrated flask sample collection system for greenhouse gas measurements, *Atmospheric Measurement Techniques*, *5*(9), 2321-2327.

Turnbull, J. C., J. B. Miller, S. J. Lehman, P. P. Tans, R. J. Sparks, and J. Southon (2006), Comparison of 14CO2, CO, and SF6 as tracers for recently added fossil fuel CO2in the atmosphere and implications for biological CO2 exchange, *Geophysical Research Letters*, *33*(1), doi:10.1029/2005gl024213.

Turnbull, J. C., C. Sweeney, A. Karion, T. Newberger, S. J. Lehman, P. P. Tans, K. J. Davis, T. Lauvaux, N. L. Miles, and S. J. Richardson (2015), Toward quantification and source sector identification of fossil fuel CO2 emissions from an urban area: Results from the INFLUX experiment, *Journal of Geophysical Research: Atmospheres*.

Vimont, I.J., Jocelyn C. Turnbull, J.C., Petrenko,V.V., Place, P.F., Karion, A., Miles, N.L., Richardson, S.J., Gurney, K, Patarasuk, R., Sweeney, C., Vaughn, B.H., White, J.W.C. Carbon monoxide isotopic measurements in Indianapolis constrain urban source isotopic signatures and support mobile fossil fuel emissions as the dominant wintertime CO source, Elem Sci Anth, 5:63, doi:10.1525/elementa.136.

von Schneidemesser, E., P. S. Monks, and C. Plass-Duelmer (2010), Global comparison of VOC and CO observations in urban areas, *Atmospheric Environment*, *44*(39), 5053-5064, doi:10.1016/j.atmosenv.2010.09.010.

Wagner, P., and W. Kuttler (2014), Biogenic and anthropogenic isoprene in the near-surface urban atmosphere - A case study in Essen, Germany, *Sci. Total Environ.*, *475*, 104-115, doi:10.1016/j.scitotenv.2013.12.026.

Warneke, C., et al. (2010), Biogenic emission measurement and inventories determination of biogenic emissions in the eastern United States and Texas and comparison with biogenic emission inventories, *J. Geophys. Res.-Atmos.*, *115*, 21, doi:10.1029/2009jd012445.

Warneke, C., et al. (2013), Photochemical aging of volatile organic compounds in the Los Angeles basin: Weekday-weekend effect, *J. Geophys. Res.-Atmos.*, *118*(10), 5018-5028, doi:10.1002/jgrd.50423.

Warneke, C., et al. (2007), Determination of urban volatile organic compound emission ratios and comparison with an emissions database, *J. Geophys. Res.-Atmos.*, *112*(D10), 13, doi:10.1029/2006jd007930.

Zobitz, J. M., J. P. Keener, H. Schnyder, and D. R. Bowling (2006), Sensitivity analysis and quantification of uncertainty for isotopic mixing relationships in carbon cycle research, *Agric. For. Meteorol.*, *136*(1-2), 56-75, doi:10.1016/j.agrformet.2006.01.003.

Atmos. Chem. Phys. Discuss., https://doi.org/10.5194/acp-2018-506
Manuscript under review for journal Atmos. Chem. Phys.
Discussion started: 22 June 2018

Atmospheric Chemistry and Physics Discussions

Tables and Figures

Table 1: Sources of CO, their isotopic values, and the CO sink. Adapted from Brenninkmeijer et al. (1999), Gros et al. (2001), and Duncan et al. (2007)

Isotopic Sources and Sinks				
Source/Sink	**$\delta^{13}C$ (VPDB)**	**Uncertainty**	**$\delta^{18}O$ (VSMOW)**	**Uncertainty**
Global Sources				
Fossil Fuel Combustion	-27.5‰	≤1‰	23.5‰	≤1‰
Biomass Burning	-22.9‰	1-3‰	17.15‰	1-3‰
CH_4 Oxidation	-52.6‰	1-3‰	0‰	>3‰
VOC Oxidation	-32‰	1-3‰	0‰	>3‰
CO Oxidation by OH Fractionation Factors	5‰	unknown	-10‰	unknown

Atmos. Chem. Phys. Discuss., https://doi.org/10.5194/acp-2018-506
Manuscript under review for journal Atmos. Chem. Phys.
Discussion started: 22 June 2018

Atmospheric Chemistry and Physics Discussions

Table 2: CH_4 and CO deviations caused by oxidation of CH_4 to CO, and oxidation of CO to CO_2 by OH. Assumed [OH] = $2x10^7$ molec cm^{-3} (Park et al., 2011). CO yield from oxidation of CH_4 taken from Grant et al. (2010).

Species	k_{OH} (cm^3 $molec^{-1}$ sec^{-1})	k_{O3} (cm^3 $molec^{-1}$ sec^{-1})	k_{NO3} (cm^3 $molec^{-1}$ sec^{-1})	Estimated Mole Fraction (nmol:mol)	γ_{OH} (%C)	Molec CO per molec VOC	Yield OH (nmol:mol)	Yield O_3 (nmol:mol)	Yield NO_3 (nmol:mol)	Total CO (nmol:mol)	$\Delta\delta^{13}C$ (‰)	$\Delta\delta^{18}O$ (‰)
Methane	6.40E-15		1.00E-18	1930	0.96	0.96	1.4	0	0.005	1.4	-0.21	-0.04
CO	1.44E-13		N/A	166	N/A	N/A	2.4	N/A	N/A	2.4	-0.08	0.17

Atmos. Chem. Phys. Discuss., https://doi.org/10.5194/acp-2018-506
Manuscript under review for journal Atmos. Chem. Phys.
Discussion started: 22 June 2018

Atmospheric Chemistry and Physics Discussions

Date	Temp (°C)	Weather	Used	~ Mean Wind Speed (MPH)	Mean Wind Speed (ms^{-1})	Wind Direction	Notes
8/27/13	32.2	Scattered clouds	yes	7	3.13	220-270	Good Sample
5/27/14	27.8	few clouds	yes	8	3.58	200-240	Good Sample
5/28/14	27.2	few clouds	yes	7	3.13	200-280	Good Sample
6/3/14	28.3	Scattered clouds	yes	12	5.36	220-270	Good Sample
8/13/14	25	few clouds	yes	10	4.47	240-310	3-5 for most of the morning, picking up a couple hours before the sample
5/5/15	26.7	Scattered clouds	yes	12	5.36	180-260	Good Sample
5/15/15	25	few clouds	yes	13	5.81	180-220	Good Sample
7/6/15	27.8	few clouds	yes	8	3.58	140-240	140 direction was very early. Mostly in the 200's for the hours ahead of the sample
7/25/15	28.3	scattered	yes	8	3.58	200-270	Good Sample
7/29/15	32.2	scattered	yes	6	2.68	200-290	Good Sample
8/1/13	27.6	Overcast AM, clearing as day goes on	yes	8	3.58	270-300	Good Sample
8/2/13	27.2	Scattered clouds all day	yes	16	7.15	190-230	Good Sample
7/27/13	23.3	Overcast AM, clearing as day goes on	yes	10	4.47	210-250	Good Sample
5/17/14	11.1	overcast	yes	8	3.58	280-350	Good Sample
8/12/14	20.6	rain/overcast	yes	15	6.70	270-280	Good Sample
5/22/15	21.7	clear	yes	10	4.47	220-270	Good Sample
8/19/14	28.9	Scattered clouds	no	10	4.47	190-240	Low wind for the morning, picking up just before sample
6/5/15	28.9	Scattered clouds	no	5	2.23	0-280	Low wind in morning, 9 ish at the time of sample, but probably not a well mixed sample
7/14/15	30	Scattered clouds/rain before dawn	no	12	5.36	170-260	thunderstorms 1-4 am
7/17/15	31.7	scattered	no	11	4.92	200-220	thunderstorms directly after the sample taken, possible there was mixing during sample?
5/12/14	25.6	Scattered clouds	no	14	6.26	10-220	highly variable wind direction througout morning. May not have sampled background
7/29/14	22.8	Scattered clouds	no	5	2.23	280-369	Wind at 8-9 mph at collection, but very calm in the morning.
7/30/14	25.6	Scattered clouds	no	7	3.13	240-260	calm in the morning, low winds
5/16/14	11.1	Scattered, raining all day	no	10	4.47	110-240	15 mph wind at time of sampling, but very calm several hours before.
6/8/15	21.1	rain/overcast	no	15	6.70	180-300	Thunderstorm
8/20/14	27.2	overcast/thunderstorm	no	6	2.68	230-290	Thunderstorm
8/21/14	27.8	scattered/thunderstroms in morning	no	3	1.34	190-200	very calm at time of sample, calm in the hours preceeding the sample
7/29/13	23.9	Scattered clouds all day	no	5	2.23	210-280	calm in am, no wind. Then picking up to 9-10 mph before sample and during sample
8/7/13	27.2	Overcast AM, broken clouds	no	8	3.58	180-220	calm in am, no wind. Then picking up to 9-10 mph before sample and during sample
8/22/14	27.8	Scattered clouds/rain in am	no	4	1.79	0-250	low wind, very variable wind conditions
6/30/15	26.1	scattered/rain/overcast in morning	no	8	3.58	210-270	thunderstorms after sample, could have been brewing ahead of sample, rain as well.

Table 3: Summary of the meteorological conditions during the samples taken during this study. The used column denotes which samples were used in this study.

Atmos. Chem. Phys. Discuss., https://doi.org/10.5194/acp-2018-506
Manuscript under review for journal Atmos. Chem. Phys.
Discussion started: 22 June 2018

Atmospheric Chemistry and Physics Discussions

VOC	k_{OH} ($cm^3 molec^{-1} sec^{-1}$)	k_{O3} ($cm^3 molec^{-1} sec^{-1}$)	k_{NO3} ($cm^3 molec^{-1} sec^{-1}$)	Emission Ratio (pmol:nmol)	Estimated Mole Fraction (pmol:mol)	γ_{OH} (%C)	Molec CO per molec VOC	Yield OH (nmol:mol)	Yield O_3 (nmol:mol)	Yield NO_3 (nmol:mol)	Total CO (nmol:mol)
Anthropogenic											
Ethane	2.50E-13			13.7	267	0.39	0.78	0.01	0	0	0.01
Propane	1.11E-12			18.7	365	0.05	0.15	0.01	0	0	0.01
i-Butane	2.30E-12			3.49	68	0.21	0.84	0.01	0	0	0.01
n-Butane	9.20E-13			6.28	122	0.21	0.84	0.01	0	0	0.01
i-Pentane	3.90E-12			8.9	174	0.21	1.05	0.07	0	0	0.07
n-Pentane	2.40E-12			3.64	71	0.21	1.05	0.02	0	0	0.02
n-Hexane	5.30E-12			1.06	21	0.21	1.26	0.01	0	0	0.01
n-Heptane	7.20E-12			0.4	8	0.21	1.47	0.01	0	0	0.01
Benzene**	1.00E-12			N/A	80	0.23	1.38	0.01	0	0	0.01
Toluene**	5.70E-12			N/A	140	0.35	2.45	0.17	0	0	**0.17**
Ethene	9.42E-12	1.60E-18		8.07	157	0.82	1.64	0.17	0.01	0	**0.17**
Propene	2.90E-11	1.00E-17		1.39	27	0.65	1.95	0.05	0.02	0	0.05
1-Butene	3.14E-11			0.14	3	0.48	1.92	0.01	0	0	0.01
t-2-Butene	5.30E-11			0.02	0.4	0.51	2.04	0.001	0	0	0.00
Acetelyne	7.80E-13	1.00E-20		7.12	139	0.6***	1.2	0.01	0	0	0.01
Acetone**	1.80E-13		6.40E-15	N/A	2110	0.46***	1.38	0.06	0	0.011	0.09
Biogenics											
Isoprene*	1.00E-10	1.27E-17		N/A	750	0.61	3.05	2.29	0.83	0	**2.35**
Methanol*	9.30E-13			N/A	2690	0.98	2.94	0.81	0	0	**0.81**
α- Pinene**	5.37E-11	9.00E-17		N/A	500	0.23	2.3	1.15	0.87	0	**1.38**
β-Pinene**	1.00E-10			N/A	500	0.19	1.9	0.95	0	0	**0.95**
										Total CO from VOC oxidation	**6.15**

*: Mole fractions taken from Jordan et al. (2009). See text for details
** Mole fractions calculated using emission ratios relative to isoprene from Duncan et al. (2007). See text for details
***: yields not available in Grant et al. (2010). Taken from Altshueller, 1991. Likely that yields are underestimated (Grant et al., 2010)

Table 4: Contribution to CO from commonly studied VOC's. Assumed [OH] = $2x10^7$ molec cm^{-3} (Park et al., 2011). The reaction rates for each VOC with OH, O_3, and NO_3 (where applicable) are represented by k_{OH}, k_{O3}, and k_{NO3} respectively. The emission ratio of each anthropogenic VOC relative to CO (pmol VOC: nmol CO) are listed for species not measured at Indianapolis. The BVOC mole fractions are estimated using literature values (see text). γ_{OH} is the yield factor of CO per carbon atom in each VOC. Molecule CO per molecule VOC is the calculated CO yield for each VOC molecule oxidized. Yield OH, yield O_3, and yield NO_3 represent the number of moles of CO produced per mole of VOC oxidized for OH, O_3 and NO_3 during the transit across the city, respectively. The total CO produced by these oxidation reactions for each VOC is calculated in Total CO. The numbers in bold represent the 6 highest producing VOC's.

Atmos. Chem. Phys. Discuss., https://doi.org/10.5194/acp-2018-506
Manuscript under review for journal Atmos. Chem. Phys.
Discussion started: 22 June 2018

Atmospheric Chemistry and Physics Discussions

Table 5: Data used in this study. The table includes all three towers, and data for days not considered due to meteorological conditions (see Table 3).

Date	Latitude	Longitude	Tower Number	CO (ppb)	±1σ CO (ppb)	$\delta^{13}CO$ (‰)	±1σ δ13CO (‰)	$\delta C^{18}O$ (‰)	±1σ $\delta C^{18}O$ (‰)
7/27/2013	39.5805	-86.4207	1	128.17	0.5	-29.15	0.037	2.46	0.09
7/27/2013	39.7978	-86.0183	2	148.1	0.5	-29.29	0.037	3.80	0.09
7/27/2013	39.7833	-86.1651	3	136.95	0.5	-29.06	0.037	3.21	0.09
7/29/2013	39.7978	-86.0183	2	150.41	0.5	-30.81	0.037	4.12	0.09
7/29/2013	39.5805	-86.4207	1	122.94	0.5	-28.53	0.037	2.87	0.09
7/29/2013	39.7833	-86.1651	3	131.39	0.5	-28.49	0.037	4.02	0.09
8/1/2013	39.7978	-86.0183	2	128.95	0.5	-29.84	0.037	3.09	0.09
8/1/2013	39.5805	-86.4207	1	116.62	0.5	-28.68	0.037	6.96	0.09
8/1/2013	39.7833	-86.1651	3	125.09	0.5	-29.66	0.037	2.44	0.09
8/2/2013	39.7978	-86.0183	2	147.92	0.5	-30.18	0.037	3.84	0.09
8/2/2013	39.5805	-86.4207	1	133.94	0.5	-30.43	0.037	3.31	0.09
8/2/2013	39.7833	-86.1651	3	159.74	0.5	-29.82	0.037	5.55	0.09
8/7/2013	39.7978	-86.0183	2	138.14	0.5	-32.28	0.037	4.87	0.09
8/7/2013	39.5805	-86.4207	1	135.21	0.5	-32.26	0.037	5.42	0.09
8/7/2013	39.7833	-86.1651	3	165.94	0.5	-30.68	0.037	7.34	0.09
8/27/2013	39.7978	-86.0183	2	165.66	0.5	-32.03	0.037	4.23	0.09
8/27/2013	39.5805	-86.4207	1	149.58	0.5	-31.78	0.037	4.21	0.09
8/27/2013	39.7833	-86.1651	3	159.21	0.5	-31.55	0.037	4.17	0.09
5/12/2014	39.7833	-86.1651	3	142.6	0.5	-28.87	0.175	5.09	0.23
5/12/2014	39.5805	-86.4207	1	127.24	0.5	-28.54	0.175	4.69	0.23
5/12/2014	39.7978	-86.0183	2	136.74	0.5	-28.44	0.175	3.92	0.23
5/16/2014	39.7833	-86.1651	3	160.4	0.5	-26.40	0.175	6.82	0.23
5/16/2014	39.5805	-86.4207	1	132.38	0.5	-26.21	0.175	4.65	0.23
5/16/2014	39.7978	-86.0183	2	152.71	0.5	-26.36	0.175	6.57	0.23
5/17/2014	39.7833	-86.1651	3	150.14	0.5	-26.01	0.175	6.54	0.23
5/17/2014	39.5805	-86.4207	1	131.46	0.5	-25.91	0.175	4.33	0.23
5/17/2014	39.7978	-86.0183	2	152.26	0.5	-26.56	0.175	6.20	0.23
5/27/2014	39.7833	-86.1651	3	156.1	0.5	-29.66	0.175	4.70	0.23
5/27/2014	39.5805	-86.4207	1	139.62	0.5	-29.92	0.175	3.67	0.23
5/27/2014	39.7978	-86.0183	2	149.96	0.5	-29.40	0.175	3.63	0.23
5/28/2014	39.7833	-86.1651	3	161.74	0.5	-29.56	0.175	4.79	0.23
5/28/2014	39.5805	-86.4207	1	128.88	0.5	-29.45	0.175	3.33	0.23
5/28/2014	39.7978	-86.0183	2	141.4	0.5	-29.32	0.175	3.25	0.23
6/3/2014	39.7833	-86.1651	3	138.13	0.5	-28.73	0.175	4.43	0.23
6/3/2014	39.5805	-86.4207	1	127.78	0.5	-28.71	0.175	3.99	0.23
6/3/2014	39.7978	-86.0183	2	141.02	0.5	-27.64	0.175	8.98	0.23

Atmos. Chem. Phys. Discuss., https://doi.org/10.5194/acp-2018-506
Manuscript under review for journal Atmos. Chem. Phys.
Discussion started: 22 June 2018

Atmospheric Chemistry and Physics Discussions

7/29/2014	39.5805	-86.4207	1	140.21	0.5	-29.29	0.204	4.18	0.50
7/29/2014	39.7833	-86.1651	3	164.6	0.5	-29.75	0.204	4.05	0.50
7/29/2014	39.7978	-86.0183	2	163.99	0.5	-29.89	0.204	3.91	0.50
7/30/2014	39.5805	-86.4207	1	148.66	0.5	-29.60	0.204	4.38	0.50
7/30/2014	39.5805	-86.4207	1	141.25	0.5	-29.49	0.204	3.29	0.50
7/30/2014	39.5805	-86.4207	1	149.63	0.5	-27.30	0.204	6.32	0.50
7/30/2014	39.5805	-86.4207	1	151.88	0.5	-28.80	0.204	6.17	0.50
7/30/2014	39.5805	-86.4207	1	153.57	0.5	-30.24	0.204	3.48	0.50
7/30/2014	39.7833	-86.1651	3	348.35	0.5	-28.16	0.204	10.54	0.50
7/30/2014	39.7833	-86.1651	3	221.51	0.5	-29.29	0.204	7.58	0.50
7/30/2014	39.7833	-86.1651	3	274.91	0.5	-28.13	0.204	10.06	0.50
7/30/2014	39.7833	-86.1651	3	176.84	0.5	-29.73	0.204	4.44	0.50
7/30/2014	39.7833	-86.1651	3	170.86	0.5	-29.52	0.204	5.47	0.50
7/30/2014	39.7978	-86.0183	2	151.14	0.5	-30.17	0.204	1.88	0.50
7/30/2014	39.7978	-86.0183	2	149.79	0.5	-29.76	0.204	3.08	0.50
7/30/2014	39.7978	-86.0183	2	161.59	0.5	-29.13	0.204	4.84	0.50
7/30/2014	39.7978	-86.0183	2	215.73	0.5	-29.36	0.204	7.97	0.50
7/30/2014	39.7978	-86.0183	2	178.48	0.5	-30.07	0.204	4.79	0.50
8/12/2014	39.7833	-86.1651	3	182.91	0.5	-29.58	0.291	4.68	0.49
8/12/2014	39.7978	-86.0183	2	191.54	0.5	-29.44	0.291	4.09	0.49
8/12/2014	39.5805	-86.4207	1	166.58	0.5	-29.32	0.291	4.56	0.49
8/13/2014	39.7833	-86.1651	3	198.59	0.5	-29.00	0.291	5.49	0.49
8/13/2014	39.7978	-86.0183	2	216.07	0.5	-29.51	0.291	4.13	0.49
8/13/2014	39.5805	-86.4207	1	192.27	0.5	-29.48	0.291	3.41	0.49
8/19/2014	39.7833	-86.1651	3	175.91	0.5	-30.84	0.291	5.70	0.49
8/19/2014	39.7978	-86.0183	2	160.48	0.5	-30.63	0.291	3.80	0.49
8/19/2014	39.5805	-86.4207	1	154.36	0.5	-31.36	0.291	4.26	0.49
8/20/2014	39.7833	-86.1651	3	148.53	0.5	-30.48	0.291	5.27	0.49
8/20/2014	39.7978	-86.0183	2	129.24	0.5	-30.80	0.291	4.28	0.49
8/20/2014	39.5805	-86.4207	1	119.46	0.5	-30.61	0.291	6.10	0.49
8/21/2014	39.7833	-86.1651	3	156.87	0.5	-31.77	0.291	5.64	0.49
8/21/2014	39.7978	-86.0183	2	154.49	0.5	-31.71	0.291	5.47	0.49
8/21/2014	39.5805	-86.4207	1	127.44	0.5	-33.19	0.291	5.25	0.49
8/22/2014	39.7833	-86.1651	3	157.19	0.5	-31.08	0.291	7.43	0.49
8/22/2014	39.7978	-86.0183	2	158.55	0.5	-30.97	0.291	6.57	0.49
8/22/2014	39.5805	-86.4207	1	112.36	0.5	-31.77	0.291	5.43	0.49
5/5/2015	39.7978	-86.0183	2	157.99	0.5	-28.18	0.31	5.59	0.34
5/5/2015	39.5805	-86.4207	1	146.94	0.5	-28.14	0.31	4.88	0.34
5/5/2015	39.7833	-86.1651	3	169.95	0.5	-27.77	0.31	6.38	0.34
5/15/2015	39.7978	-86.0183	2	173.37	0.5	-28.98	0.31		0.34

Atmos. Chem. Phys. Discuss., https://doi.org/10.5194/acp-2018-506
Manuscript under review for journal Atmos. Chem. Phys.
Discussion started: 22 June 2018

Atmospheric Chemistry and Physics Discussions

5/15/2015	39.5805	-86.4207	1	157.3	0.5	-29.64	0.31	4.86	0.34
5/15/2015	39.7833	-86.1651	3	188.53	0.5	-28.50	0.31	7.47	0.34
5/18/2015	39.7978	-86.0183	2	142.23	0.5	-29.32	0.31	4.94	0.34
5/18/2015	39.5805	-86.4207	1	125.93	0.5	-29.54	0.31	3.36	0.34
5/22/2015	39.7978	-86.0183	2	157.54	0.5	-26.48	0.31	7.42	0.34
5/22/2015	39.5805	-86.4207	1	145.09	0.5	-26.78	0.31	5.96	0.34
5/22/2015	39.7833	-86.1651	3	160.71	0.5	-26.68	0.31	6.48	0.34
6/5/2015	39.7978	-86.0183	2	151.26	0.5	-28.74	0.31	5.96	0.34
6/5/2015	39.5805	-86.4207	1	143.78	0.5	-29.31	0.31	4.59	0.34
6/5/2015	39.7833	-86.1651	3	175.26	0.5	-28.14	0.31	7.41	0.34
6/8/2015	39.7978	-86.0183	2	152.65	0.5	-28.27	0.31	7.50	0.34
6/8/2015	39.5805	-86.4207	1	113.92	0.5	-30.15	0.31	0.71	0.34
6/8/2015	39.7833	-86.1651	3	171.44	0.5	-27.96	0.31	8.30	0.34
6/30/2015	39.7978	-86.0183	2	245.75	0.5	-29.29	0.252	5.09	0.73
6/30/2015	39.7833	-86.1651	3	240.22	0.5	-29.70	0.252	5.85	0.73
6/30/2015	39.5805	-86.4207	1	233.09	0.5	-29.41	0.252	4.90	0.73
7/6/2015	39.7978	-86.0183	2	264.26	0.5	-29.54	0.252	5.25	0.73
7/6/2015	39.7833	-86.1651	3	263.22	0.5	-29.75	0.252	6.06	0.73
7/6/2015	39.5805	-86.4207	1	221.56	0.5	-30.13	0.252	4.49	0.73
7/14/2015	39.7978	-86.0183	2	151.26	0.5	-30.28	0.252	2.86	0.73
7/14/2015	39.7833	-86.1651	3	149.07	0.5	-30.34	0.252	3.61	0.73
7/14/2015	39.5805	-86.4207	1	154.69	0.5	-30.74	0.252	3.32	0.73
7/17/2015	39.7978	-86.0183	2	149.6	0.5	-32.83	0.252	4.02	0.73
7/17/2015	39.7833	-86.1651	3	189.17	0.5	-32.54	0.252	5.12	0.73
7/17/2015	39.5805	-86.4207	1	149.22	0.5	-34.16	0.252	2.24	0.73
7/25/2015	39.7978	-86.0183	2	216.11	0.5	-29.77	0.252	4.50	0.73
7/25/2015	39.7833	-86.1651	3	212.78	0.5	-30.37	0.252	3.13	0.73
7/25/2015	39.5805	-86.4207	1	196.57	0.5	-30.84	0.252	3.61	0.73
7/29/2015	39.7978	-86.0183	2	155.67	0.5	-32.43	0.252	4.11	0.73
7/29/2015	39.7833	-86.1651	3	152	0.5	-32.66	0.252	2.85	0.73
7/29/2015	39.5805	-86.4207	1	135.3	0.5	-33.50	0.252	1.39	0.73

Atmos. Chem. Phys. Discuss., https://doi.org/10.5194/acp-2018-506
Manuscript under review for journal Atmos. Chem. Phys.
Discussion started: 22 June 2018

Atmospheric Chemistry and Physics Discussions

Figure 1: Satellite image of Indianapolis with the tower locations marked. Note the foliage around towers 1 and 2.

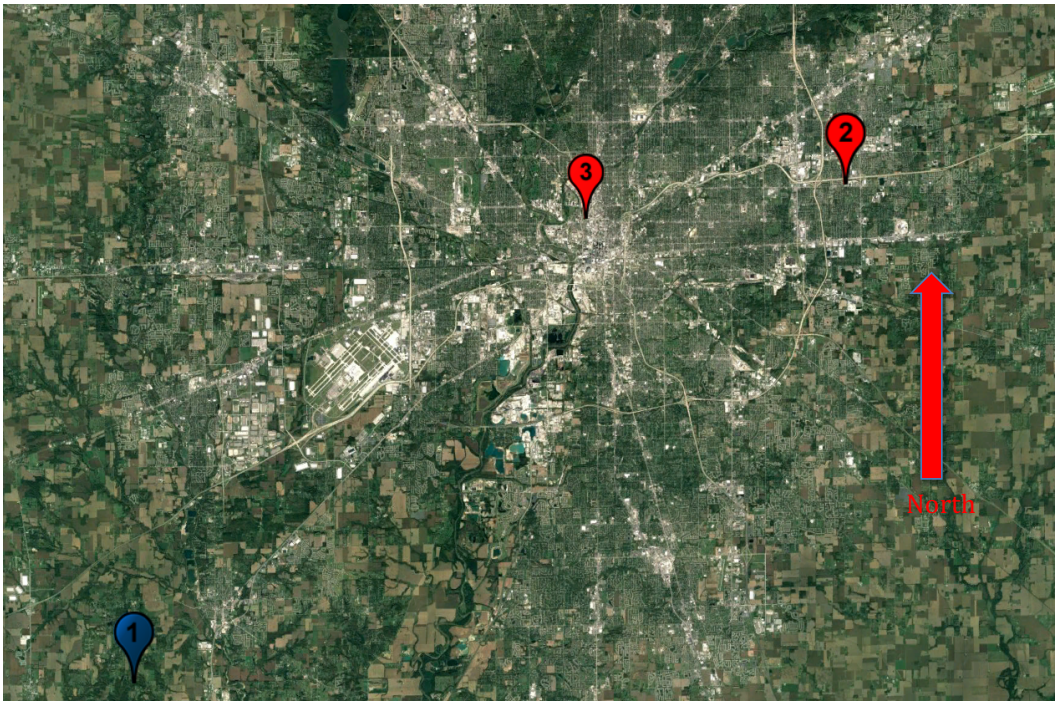

Atmos. Chem. Phys. Discuss., https://doi.org/10.5194/acp-2018-506
Manuscript under review for journal Atmos. Chem. Phys.
Discussion started: 22 June 2018

Atmospheric Chemistry and Physics Discussions

Figure 2: Map of the INFLUX network (Miles et al., 2017)

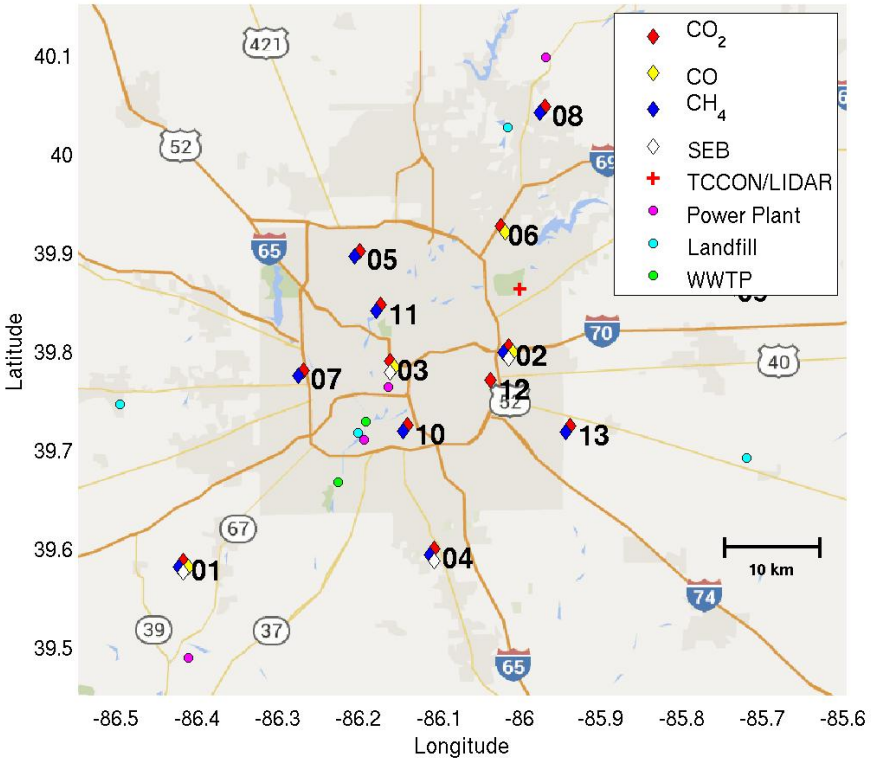

Atmos. Chem. Phys. Discuss., https://doi.org/10.5194/acp-2018-506
Manuscript under review for journal Atmos. Chem. Phys.
Discussion started: 22 June 2018

Atmospheric Chemistry and Physics Discussions

Figure 3: Reproduced from Figure 1 in Turnbull et al. (2015) showing the footprints of the INFLUX tower network. This illustrates the common zones of influence for each tower. The samples for this study were taken when the winds were out of the western sector. Thus, the footprints of interest for each tower are those to the western side of towers 1,2, and 3.

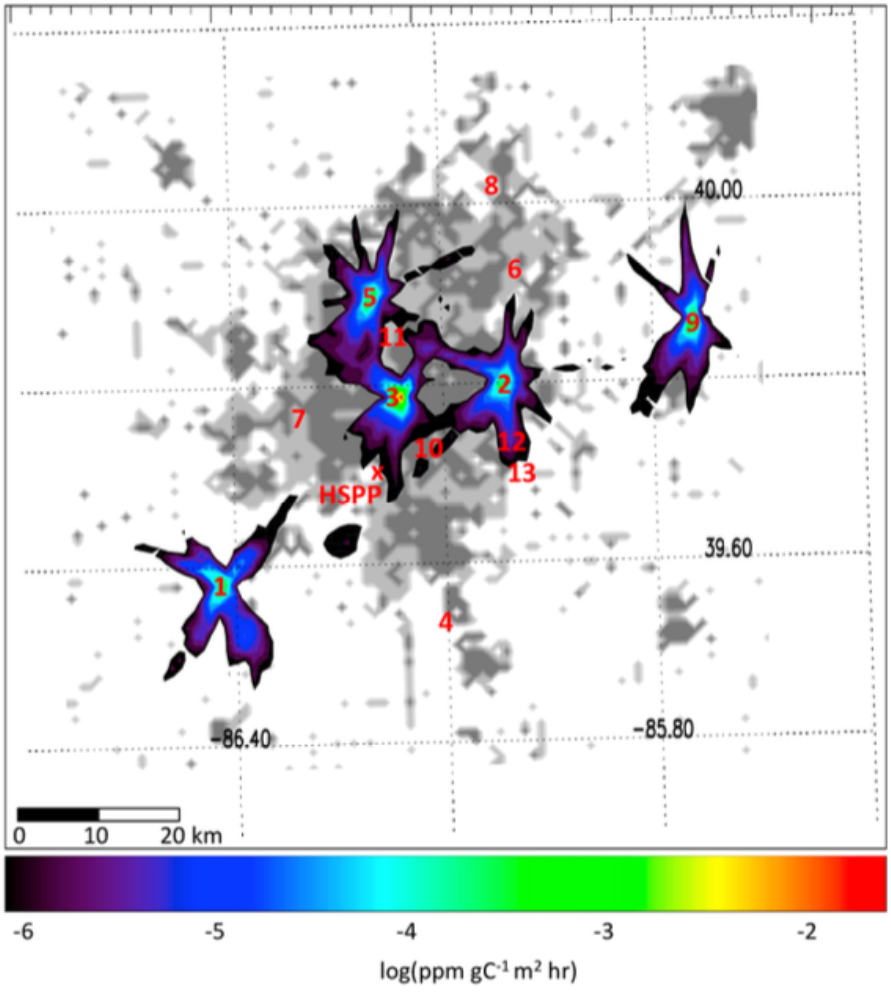

Figure 1. Map of the Indianapolis Metropolitan Area and surrounds. Grey background shading indicates urban density from low (white) to high (dark grey) from the 2006 U.S. National Land Cover Database [*Fry et al.*, 2011]. Locations of the INFLUX towers and the Harding Street Power Plant (HSPP) are shown in red. The modeled aggregate surface influence functions for midafternoon in October 2012 for Towers 1, 2, 3, 5, and 9 are overlaid using the color scale shown. All wind directions are included in the modeled aggregate influence functions. The "star" shape of the influence functions is a consequence of the dominant wind directions over the 1 month modeled period.

Atmos. Chem. Phys. Discuss., https://doi.org/10.5194/acp-2018-506
Manuscript under review for journal Atmos. Chem. Phys.
Discussion started: 22 June 2018

Atmospheric Chemistry and Physics Discussions

Figure 4: Regression plots to analyze the δ_s of each tower. Tower 2 is in red, Tower 3 is in blue. Both regression slopes represent the δ value of the urban enhancements.

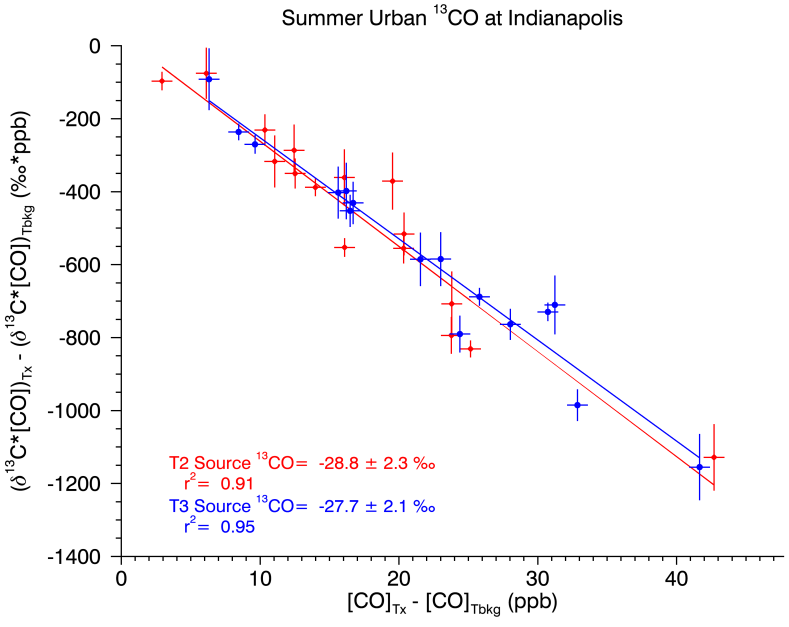

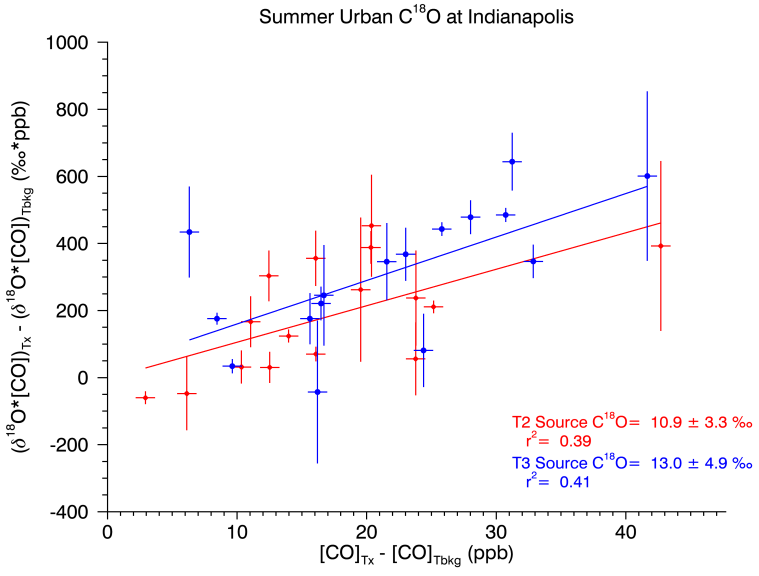

Atmos. Chem. Phys. Discuss., https://doi.org/10.5194/acp-2018-506
Manuscript under review for journal Atmos. Chem. Phys.
Discussion started: 22 June 2018

Atmospheric Chemistry and Physics Discussions

Figure 5: Time series of the two years of data measured at Indianapolis, reproduced from Vimont et al. (2017).